iScience

CellPress

Article

Recall Responses from Brain-Resident Memory CD8$^+$ T Cells (bT$_{RM}$) Induce Reactive Gliosis

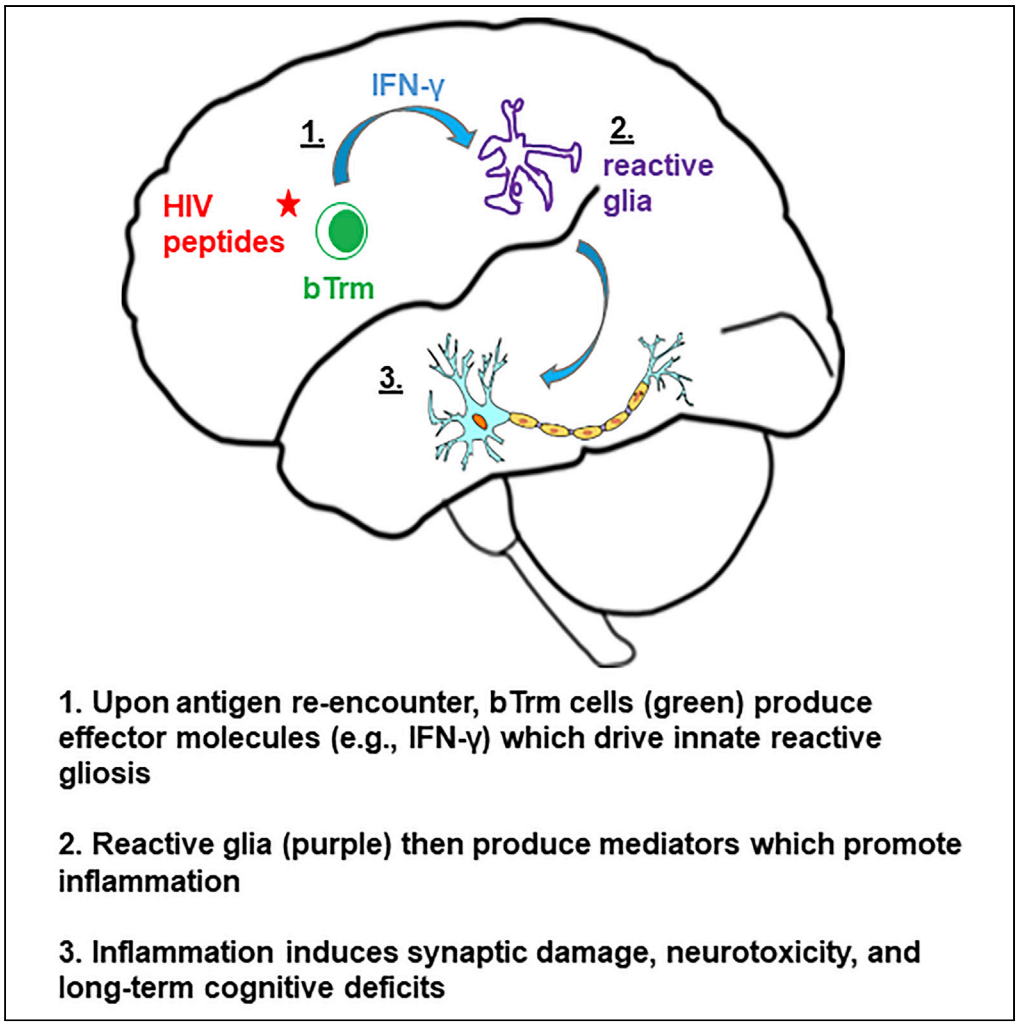

Sujata Prasad, Shuxian Hu, Wen S. Sheng, Priyanka Chauhan, James R. Lokensgard

loken006@umn.edu

HIGHLIGHTS

Heterologous prime-CNS boost induced HIV-1-specific bT$_{RM}$, which persisted long term

Recall responses from HIV-specific bT$_{RM}$ induced tissue-wide reactive gliosis

bT$_{RM}$ induced-reactive gliosis likely has cumulative neurotoxic consequences

Prasad et al., iScience *20*, 512–526
October 25, 2019
https://doi.org/10.1016/j.isci.2019.10.005

iScience

CellPress

Article

Recall Responses from Brain-Resident Memory CD8$^+$ T Cells (bT$_{RM}$) Induce Reactive Gliosis

Sujata Prasad,[1] Shuxian Hu,[1] Wen S. Sheng,[1] Priyanka Chauhan,[1] and James R. Lokensgard[1,2,*]

SUMMARY

HIV-associated neurocognitive disorders (HAND) persist even during effective combination antiretroviral therapy (cART). Although the cause of HAND is unknown, studies link chronic immune activation, neuroinflammation, and cerebrospinal fluid viral escape to disease progression. In this study, we tested the hypothesis that specific, recall immune responses from brain-resident memory T cells (bT$_{RM}$) could activate glia and induce neurotoxic mediators. To address this question, we developed a heterologous prime-central nervous system (CNS) boost strategy in mice. We observed that the murine brain became populated with long-lived CD8$^+$ bT$_{RM}$, some being specific for an immunodominant Gag epitope. Recall stimulation using HIV-1 AI9 peptide administered *in vivo* resulted in microglia displaying elevated levels of major histocompatibility complex class II and programmed death-ligand 1, and demonstrating tissue-wide reactive gliosis. Immunostaining further confirmed this glial activation. Taken together, these results indicate that specific, adaptive recall responses from bT$_{RM}$ can induce reactive gliosis and production of neurotoxic mediators.

INTRODUCTION

It is currently unknown why HIV-associated neurocognitive disorders (HAND) persist despite effective viral suppression to undetectable levels in most combination antiretroviral therapy (cART)-treated individuals. Although patients on successful cART show sustained viral suppression, as indicated by routine plasma monitoring and occasional cerebrospinal fluid (CSF) monitoring, "blips" indicative of transient HIV replication are often detected with more frequent testing, as reviewed in Chen et al. (2014). A number of studies link persistent immune activation, neuroinflammation, and CSF viral escape in cART-treated individuals to increased disease progression, as well as an increased risk for HAND (Childers et al., 2008; Gisslen et al., 2005; Monteiro de Almeida et al., 2005). Interruption of cART has been associated with CSF viral escape and neuronal injury, as well as with worsened neurocognitive performance (Childers et al., 2008; Gisslen et al., 2005; Monteiro de Almeida et al., 2005). Although fulminant encephalitis is now uncommon in HIV-infected patients, biomarkers of continuing neuroinflammation in the CSF and brain, as well as neuronal injury, are frequently detected in virally suppressed individuals. Still, partial protection against HAND by successful cART does indicate some direct link to HIV replication. Persistent HIV infection and reactivation from central nervous system (CNS) reservoirs, even if intermittent, appears likely in cART-experienced patients (Stam et al., 2013). Brain infection may also be re-seeded through blood or through recently described meningeal lymphatics (Lamers et al., 2016). In addition, evidence for the involvement of CD8$^+$ T cells, especially through production of interferon (IFN)-γ, in CNS pathogenesis in patients who received cART continues to mount (Schrier et al., 2015). Therefore, CSF viral escape and the associated production of viral antigen (Ag), as well as its generation of subsequent adaptive, recall responses by brain-resident CD8$^+$ T cells to control viral spread, may induce neuroinflammation that drives bystander CNS injury.

Resolution of adaptive immune responses and generation of immunological memory is an essential process to confer long-term protective immunity, particularly in tissues like the brain. The presence of CD8$^+$ T cells in post-mortem brains of HIV-infected patients, as well as in the brains of animal models, is well documented (Ganesh et al., 2016; Graham et al., 2011; Grauer et al., 2015; Ho et al., 2013; Kowarik et al., 2014; Marcondes et al., 2007; Schrier et al., 2015). Recent studies have demonstrated that following clearance of many acute viral infections, CD8$^+$ T lymphocytes generate a population of long-lived, non-recirculating tissue-resident memory T cells (T$_{RM}$) in non-lymphoid tissue, and it is becoming increasingly clear that these T$_{RM}$ play critical roles in controlling re-encountered pathogens and accelerating the process

[1]Neurovirology Laboratory, Department of Medicine, University of Minnesota, 3-107 Microbiology Research Facility, 689 23rd Avenue S.E., Minneapolis, MN 55455, USA

[2]Lead Contact

*Correspondence: loken006@umn.edu

https://doi.org/10.1016/j.isci.2019.10.005

of clearance (Mackay et al., 2013; Masopust et al., 2010; Park and Kupper, 2015; Schenkel and Masopust, 2014). It is well established that during acute viral infection, most pathogens are rapidly cleared by the generation of a large number of short-lived effector T cells (SLEC), which die via apoptosis once cognate Ag is cleared. Simultaneously, the T cell response is also triggered to generate a defined subset identified as memory precursor effector cells (MPEC). These MPEC begin to develop into a T_{RM} phenotype shortly after infection. Recent work by several groups provides evidence that there is a clear distinction between terminal effector and memory cells based on heterogeneity in expression of killer cell lectin-like receptor G1 (KLRG1) (Bengsch et al., 2007; Kaech and Wherry, 2007; Yuzefpolskiy et al., 2015).

We have recently characterized brain-infiltrating T cells that persist within the CNS after acute murine cytomegalovirus (MCMV) infection (Prasad et al., 2015). We have also shown that these brain $CD8^+$ T cell populations shift from SLEC that clear infection to MPEC that protect against viral reactivation and re-challenge. The shift of prominent SLEC populations to MPEC populations is concomitant with transition from acute through chronic phases of infection. T_{RM} are characterized by their non-recirculating, resident nature in tissues. It has been well reported that T_{RM} often express αEβ7 integrin, and integrin αE, otherwise known as CD103, is used as a marker of particular types of T_{RM}. High expression of CD103 and CD69 is a common feature of resident memory cells observed in epithelial tissue, as well as a phenotypic signature of bT_{RM} (Steinbach et al., 2016; Wakim et al., 2010; Watanabe et al., 2015; Woon et al., 2016). In contrast, effector and memory cells in circulation appear to lack expression of both CD103 and CD69 (Gebhardt and Mackay, 2012; Masopust et al., 2006). It has also been shown that CD69 expression is required for optimal formation of T_{RM} following herpes simplex virus infection in tissues such as the skin and dorsal root ganglia (Mackay et al., 2013, 2015b). In addition to $CD103^+$ and $CD69^+$ markers, T_{RM} are often reported to express CD49a. CD49a constitutes the α subunit of α1β1 integrin receptor, also known as very late Ag 1 (VLA-1) (Cheuk et al., 2017). Experiments using skin, lung, and gut show differential expression of CCR7, as well as CXCR3, which define migration properties of T cells (Mueller and Mackay, 2016; Slutter et al., 2013). Although imperfect, expression of these markers is frequently used to identify T_{RM} populations when stringent migration studies, such as parabiosis, are not feasible, reviewed in Schenkel and Masopust (2014). Finally, protection of the CNS from reinfection by lymphocytic choriomeningitis virus (LCMV) was found to depend on these brain-resident memory $CD8^+$ T cells (bT_{RM}) (Steinbach et al., 2016).

Given their significance in antiviral defense, surprisingly little is known about this brain-resident memory cell population in the context of HAND. Ag-specific lymphocytes residing within tissues are uniquely poised to respond rapidly to their cognate Ag, and T_{RM} functions extend far beyond cytotoxic T lymphocyte activity. In several infection models, it is clear that recall responses of T_{RM} to small amounts of Ag result in production of IFN-γ (McMaster et al., 2015; Steinbach et al., 2016). Furthermore, this IFN-γ production results in IFN-stimulated gene expression in surrounding cells, thereby amplifying the activation of a small number of adaptive immune cells into an organ-wide antiviral response (Ariotti et al., 2014). Similarly, activation of adaptive immune responses from T_{RM} has been shown to stimulate protective, innate responses in the LCMV model (Schenkel and Masopust, 2014). From these studies, it is clear that a small number of T_{RM} accelerate pathogen control in the event of reinfection or reactivation of latent infection by instructing tissue-resident innate immune cells, such as microglia. Yet there have been no definitive experiments to evaluate neurotoxic consequences of anti-HIV recall immune response by bT_{RM} in driving tissue-wide activation of brain-resident microglial cells, its associated neurotoxicity, and development of subsequent neurocognitive impairment. Here, we demonstrate that HIV-specific T_{RM} are elicited within brain using a heterologous prime-CNS boost strategy. We show that Ag-specific $CD8^+$ bT_{RM} are established, which recognize an immunodominant viral epitope. Subsequent recall responses to specific epitope peptides resulted in striking upregulation of major histocompatibility complex (MHC) class II (MHC-II) and programmed death-ligand 1 (PD-L1) on microglial cells, indicative of neuroinflammation. Taken together, data presented here show that recall responses from bT_{RM} can induce reactive gliosis.

RESULTS

Ag-Specific $CD8^+$ T Cells Infiltrate and Are Retained within the Brain following Priming with rAd5-p24 and CNS Boosting Using $Pr55^{Gag/Env}$ HIV-VLPs

To investigate whether recall responses from bT_{RM} can induce reactive gliosis, we first established a population of HIV-specific T cells within the murine brain using a heterologous prime-CNS boost strategy. To accomplish this, BALB/c mice were primed via tail vein injection with recombinant adenovirus vectors

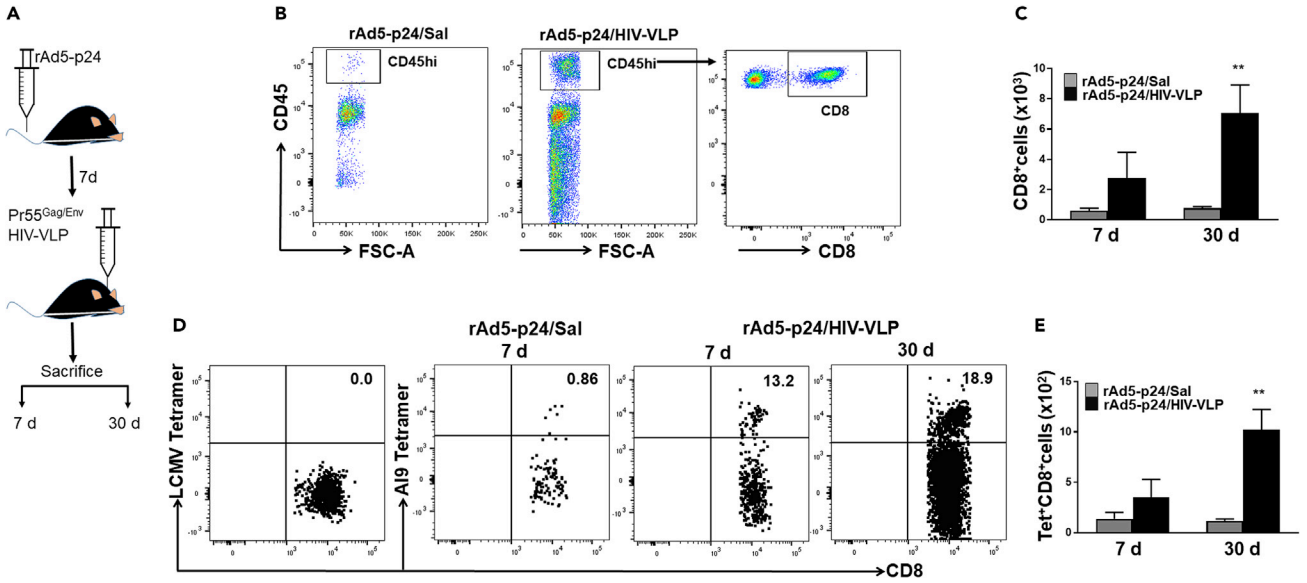

Figure 1. Lymphocyte Infiltration into the Brain and Long-Term Presence of Ag-Specific CD8$^+$ T Cells following Heterologous Prime-CNS Boost

(A) Schematic of the experimental model illustrates intravenous delivery of recombinant adenovirus vectors expressing HIV-1 p24 capsid protein (rAD5-p24), followed by a CNS-boost consisting of intracranial injection of HIV-VLPs into the striatum. BMNC were collected at 7 and 30 days post prime-boost.

(B) Flow cytometric analysis demonstrating lymphocyte infiltration and CD8$^+$ T cell retention within the brain following heterologous CNS boost.

(C) Absolute numbers of CD8$^+$ T cells were determined within brains of animals at the indicated time points.

(D) Dot plot comparing the frequencies of AI9 tetramer-specific CD8$^+$ T cells in brain tissue isolated from rAd5-p24/Sal (saline) and rAd5-p24/HIV-VLP groups.

(E) Bar graph presents absolute numbers of T cells between groups. Pooled data are presented as mean ± SD of two independent experiments using four to six animals per group per time point. **$p < 0.01$

expressing the HIV-1 p24 capsid protein (rAd5-p24). This priming step was followed by a CNS-boost using Pr55$^{Gag/Env}$ virus-like particles (HIV-VLPs) injected directly into the striatum (Figure 1A). Using immunohistochemical (IHC) staining, we first confirmed that the adenovirus construct delivered bona fide HIV-p24 protein by staining murine liver sections 7 days post-priming (Figure S1 A). We then detected increased lymphocyte trafficking into the brains of rAd5-p24-primed animals, which received an HIV-VLP CNS boost when compared with control animals that were primed, but did not receive HIV-1 Ag in the brain (Figures 1B and 1C). We observed that CD8$^+$ T cells infiltrated the brain and were present at 7 days post HIV-VLP injection, and further increased at 30 days post prime-CNS boost (Figure 1C). In addition, we used tetramer staining to confirm that AI9-specific, but not LCMV epitope-specific, CD8$^+$ T cells were present at 7 days and continued to persist until at least 30 days post prime-CNS boost (Figures 1D and 1E). We also examined the recruitment of CD4$^+$ T cells and observed an influx into the brain at 7 days following prime-CNS boost (38.3%). The frequency of CD4$^+$ T cells increased by 30 days (42.2%), similar to that observed for CD8$^+$ T cells. However, by 60 days the frequencies of both CD8$^+$ and CD4$^+$ T cells decreased (20.8% and 32.9%, respectively). In addition, as a result of AI9 *in vivo* restimulation, the frequency of CD8$^+$ T cells was elevated by 2 days post-peptide injection, whereas CD4$^+$ T cell frequency was not (Figure S2A).

Memory CD8$^+$ T Cells Are Present within the Brain following Prime-CNS Boost Strategies

To characterize HIV-specific CD8$^+$ T cells within the brain, we analyzed Ag-specific cells for phenotypic markers at both 7 and 30 days post prime-CNS boost (Figure 2A). We first determined the pattern of CD127 and KLRG1 expression on these Ag-specific cells. We observed expression of CD127 on some Ag-specific CD8$^+$ T cells during the acute phase of infection, whereas a larger fraction of AI9 tetramer$^+$ CD8$^+$ T cells displayed high CD127 expression at 30 days post prime-CNS boost (Figure 2B). In sharp contrast, KLRG1 expression was found to be 37.8% ± 3.4% among Ag-specific cells during onset of infection, whereas it decreased to 19.8% ± 2.7% at 30 days (Figures 2B and 2C). To gain insight into the diversity of T_{RM} phenotypes, we next examined the relative expression of various residency markers such as CD103, CD69, and CD49a. An increased expression of CD69 at 7 days suggested that these Ag-specific CD8$^+$

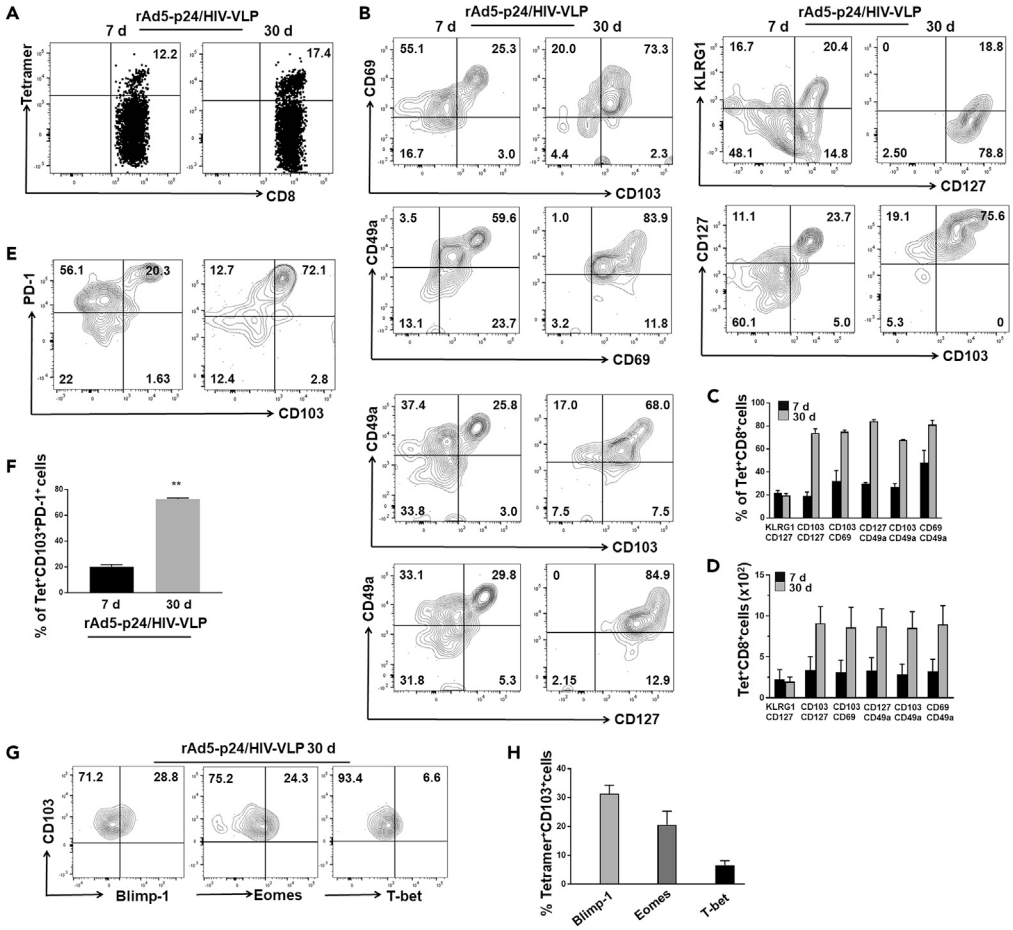

Figure 2. Phenotypic Characterization of Ag-Specific T_{RM} within the Brain

(A and B) CNS-derived lymphocytes were gated for AI9-specific $CD8^+$ T cells and analyzed for the indicated memory cell markers (CD127, CD103, CD69, CD49a), as well as the short-lived effector marker KLRG1.

(C and D) Bar graphs present pooled frequencies and number of Ag-specific cells that expressed the indicated phenotypic markers.

(E) Additional contour plots show PD-1 expression on these Ag-specific $CD103^+$ $CD8^+$ T cells at 7 and 30 days post prime-boost.

(F) Pooled data show frequency of PD-1 expression on Ag-specific $CD103^+CD8^+$ T cells at the indicated time points. $^{**}p < 0.01$.

(G) Representative plots show expression of transcription factors Blimp-1, Eomes, and T-bet at the indicated time point.

(H) Pooled data present percentage of Blimp-1, Eomes, and T-bet expression. Graph presents data combined from two separate experiments using four to six animals per group per time point.

T cells progress to an activated state. Expression of CD49a was also observed during establishment of infection. Interestingly, expression of both CD69 and CD49a remained elevated even at 30 days. Their increased co-expression was also observed during the chronic phase (81.1% ± 3.8%; Figures 2B and 2C). Moreover, high co-expression of CD69 and CD103 (74% ± 3.5%), as well as CD127 and CD103 (75% ± 1.3%), was observed. In addition, an increased proportion of Ag-specific $CD8^+$ T cells was found to co-express CD49a and CD103 (67.9% ± 0.3%), as well as CD49a and CD127 (84.2% ± 1.1%) (Figures 2B and 2C). Evaluation of various memory marker-expressing cells revealed greater numbers of T_{RM} at 30 days than at 7 days following prime-CNS boost (Figure 2D). Finally, we also observed that these Ag-specific $CD8^+CD103^+$ T cells also expressed programmed cell death (PD)-1 (72.5% ± 0.8%) (Figures 2E and 2F). Furthermore, evaluation of additional transcription factors associated with tissue residency revealed elevated levels of B lymphocyte-induced maturation protein (Blimp)-1 and eomesodermin (Eomes), whereas reduced levels of T-box expressed in T cells (T-bet) were seen at 30 days post prime-CNS boost (Figures 2G and 2H).

Effector Responses of bT_{RM}

To investigate the ability of bT_{RM} to respond to restimulation, we evaluated the production of IFN-γ and interleukin-2 (IL-2), as well as granzyme B. Analysis was performed using intracellular staining and flow cytometry following *ex vivo* stimulation with AI9 peptide, which is an immunodominant, H-$2K^d$ MHC-I-restricted T cell epitope from the p24 (65-73) capsid. Brain-derived $CD8^+CD103^+$ T_{RM} produced IFN-γ following peptide stimulation. Higher frequencies (55.8% ± 7.3%) were produced following *ex vivo* peptide stimulation when compared with unstimulated control (3.0% ± 0.43%, $p < 0.05$) (Figures 3A and 3B). We also analyzed dual cytokine production by assessing IFN-γ and IL-2 co-expression. A substantial percentage of dual IFN-γ- and IL-2-producing $CD8^+CD103^+$ T cells (30.4% ± 4.0%) was detected following peptide restimulation (Figures 3A and 3B). Increased production of tumor necrosis factor (TNF)-α was also noted in response to *ex vivo* AI9 restimulation (Figures 3C and 3D). In addition, granzyme B-expressing cells were also detected in a larger proportion (39.2% ± 3.6%) when compared with unstimulated control (8.4% ± 1.3%) (Figures 3E and 3F). Finally, we analyzed the proliferation potential of these $CD103^+CD8^+$ T cells following Ag stimulation and found that Ki67 was expressed in a significant fraction, whereas unstimulated cells displayed lower levels (35.3% ± 6.1% and 10.2% ± 1.4%, respectively) (Figures 3G and 3H).

Glial Cell Activation following Peptide Restimulation

Having observed that *ex vivo* stimulation resulted in cytokine production, we went on to determine the capacity of these viral-peptide-induced recall responses to activate glia. In these experiments, brain-derived mononuclear cells (BMNC) obtained from prime-CNS boost mice at 30 days were co-cultured with primary murine glial cells (40% microglia, 60% astrocytes) and stimulated with either the AI9 peptide or the non-specific M54 peptide epitope from MCMV. Increased transcription of proinflammatory mediators (i.e., IFN-γ, CXCL9, CXCL10, nitric oxide synthase [iNOS], and PD-1) was observed in the co-cultures after 24 h of stimulation with specific (AI9), but not non-specific (M54), T cell epitope peptides (Figure 4A). Also, elevated levels of MHC-II, PD-L1, and Iba (ionized calcium-binding adaptor molecule)-1 mRNA indicated glial cell activation in response to AI9, but not M54, peptide (Figure 4A). To specifically evaluate the role of $CD8^+$ T cells in modulating glial activation, we used positive selection to deplete this T cell population from the BMNC isolated from prime-CNS boost animals at 30 days. Depletion of $CD8^+$ T cells was confirmed using flow cytometry (Figure S2B). The sorted BMNC (i.e., with and without $CD8^+$ T cells) were then cultured with mixed glial cells, and transcription of the same proinflammatory mediators was assessed after 48 h. Depletion of $CD8^+$ T cells was found to reduce transcription of IFN-γ as well as the IFN-γ-induced chemokines CXCL9 and CXCL10. Reductions in transcription of MHC-II, PD-L1, Iba-1, iNOS, and PD-1 were also observed in the absence of $CD8^+$ T cells (Figure 4B). Also, to determine the individual contribution of each glial cell type, we assessed cytokine and chemokine production at the protein level from co-cultures of AI9-stimulated BMNC reconstituted with either primary microglial cells or primary astrocytes. ELISA results indicated that BMNC produced IFN-γ, in response to AI9 restimulation, either when cultured alone or when reconstituted with either microglia or astrocytes (Figure 4C). Elevated levels of CXCL9 (Figure 4D) and CXCL10 (Figure 4E) were found in the BMNC-glial cell co-cultures, but not from AI9-stimulated BMNC alone. Co-cultures of unstimulated BMNC (i.e., no AI9 treatment) with either microglia or astrocytes produced negligible levels of IFN-γ, CXCL9, or CXCL10 (Figure 4C–4E). Interestingly, treatment of the co-cultures with an anti-IFN-γ neutralizing antibody significantly reduced subsequent glial cell expression of CXCL9 and CXCL10 when compared with IgG isotype antibody (Figures 4F and 4G).

In vivo Recall Responses Stimulate Rapid Proliferation of HIV-Specific bT_{RM} within the Brain

It is well-established that T_{RM} respond rapidly to an Ag re-challenge (Schenkel and Masopust, 2014). Our *ex vivo* studies demonstrated that IFN-γ and IFN-γ-inducible chemokines, as well as microglial activation makers, were produced following peptide-specific stimulation. To study recall responses *in vivo*, we intracranially administered either the Ag-specific peptide AI9 or an irrelevant peptide or saline to animals at 30 days post prime-CNS boost (Figure 5A). We first found that recall activation following injection of HIV-specific peptide resulted in an increased number of AI9 tetramer$^+$ $CD8^+$ T cells within the brain (Figure 5B). This effect was specific to AI9 peptide and was not observed with irrelevant peptide (M54) or saline (Sal) (Figures 5B and 5C). We went on to determine that brain-resident $CD103^+CD8^+$ T cells expanded following *in vivo* restimulation. Ki67 staining demonstrated this increased bT_{RM} proliferation in response to AI9 restimulation relative to the control group (Figures 5D and 5E).

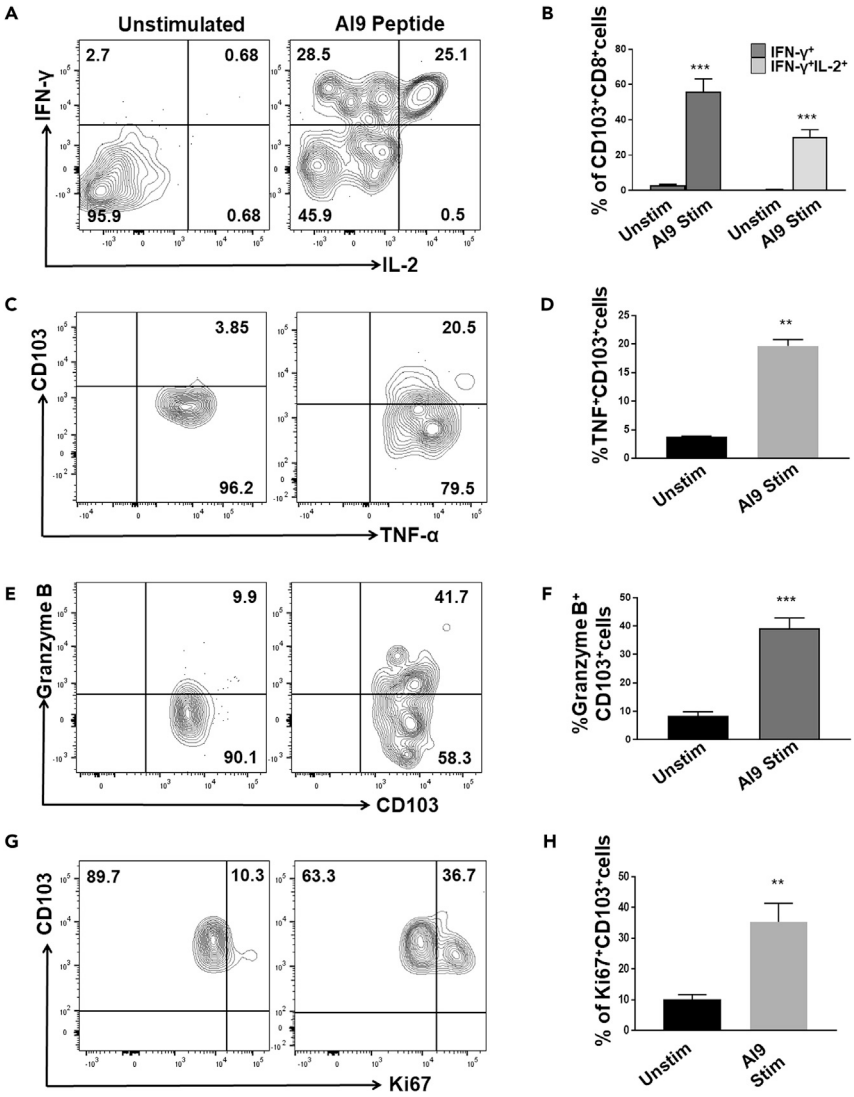

Figure 3. Ag-Specific CD103$^+$CD8$^+$ T Cells Display Recall Responses

BMNC obtained from animals at 30 days post prime-CNS boost were either restimulated *ex vivo* with AI9 peptide or left unstimulated, and intracellular staining was performed. Gated CD103$^+$CD8$^+$ T cells were assessed for cytokine production in response to peptide stimulation.

(A) Representative contour plots present expression of IFN-γ and IL-2 by CD103$^+$CD8$^+$ T cells.

(B) Bar graph of pooled data shows frequencies of IFN-γ production by CD103$^+$CD8$^+$ T cells, as well as simultaneous detection of IFN-γ and IL-2 double-producer cells.

(C) Contour plots show TNF-α production by CD103$^+$CD8$^+$ T cells.

(D) Pooled data show the frequency of TNF-α production.

(E) Representative contour plots of granzyme B show *ex vivo* production of this cytotoxic mediator in response to peptide stimulation.

(F) Data presented show percentage of granzyme B-producing CD103$^+$CD8$^+$ T cells.

(G) Contour plots following Ki67 staining show proliferation frequencies of CD103$^+$CD8$^+$ T cells, either with or without peptide stimulation.

(H) Pooled data present percentage proliferation of bT$_{RM}$.

**$p < 0.01$ and ***$p < 0.001$

Recall Responses Induce Glial Cell Activation

Having observed that T$_{RM}$ isolated from the brain produce abundant proinflammatory cytokines following AI9 peptide stimulation *ex vivo*, we next investigated the *in vivo* induction of reactive gliosis.

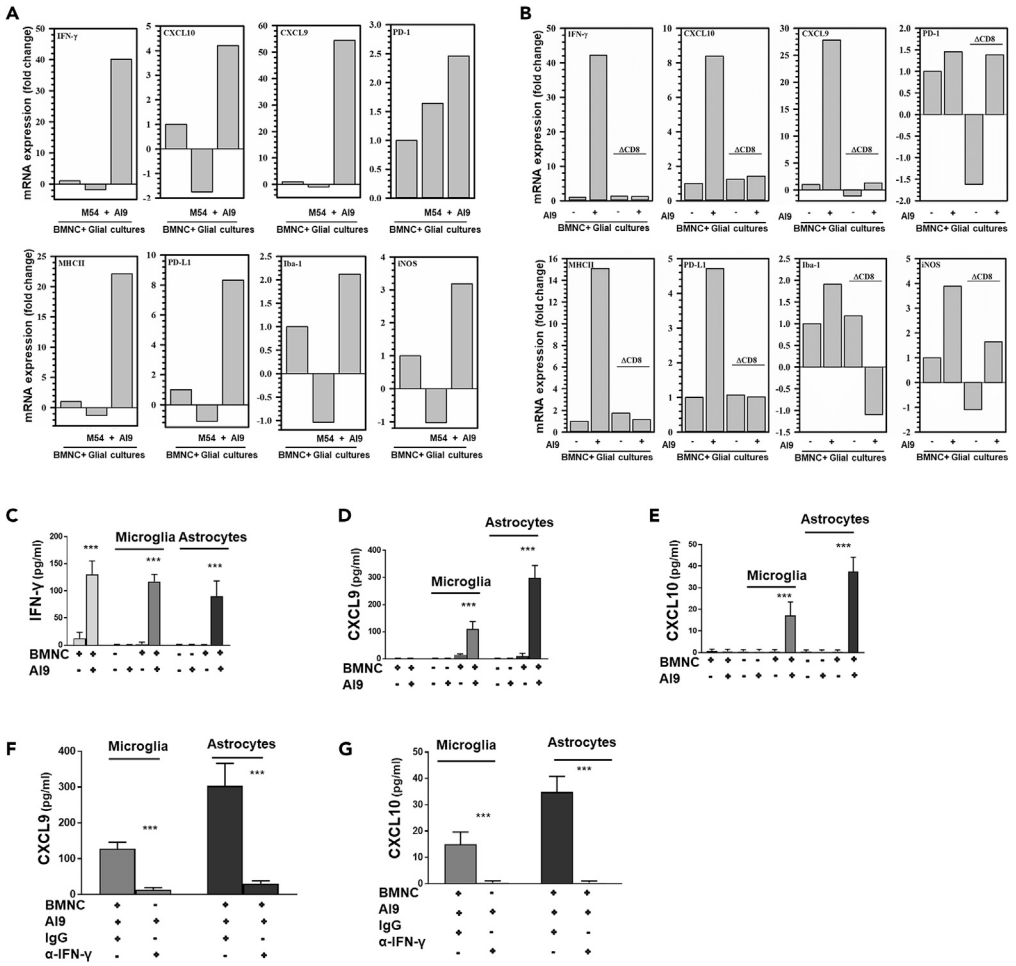

Figure 4. Specific *Ex Vivo* Peptide Restimulation of T Cells Activates Primary Glial Cells

(A) BMNC isolated from brains of 30 days post prime-boost animals were co-cultured with primary murine glial cells (40% microglia; 60% astrocytes). Cells were either treated with HIV-specific AI9 or MCMV M54 T cell epitope peptides or left untreated for 24 h. Real-time PCR data show mRNA expression levels of IFN-γ, MHC-II, PD-L1, PD-1, Iba-1, CXCL9, CXCL10, and nitric oxide synthase (iNOS) under the indicated treatment.

(B–G) (B) Cultures with or without the CD8 T cell population were either stimulated with AI9 peptide or left unstimulated for 1 h before being co-cultured with mixed glial cells (40% microglia; 60% astrocytes) for 24 h. qPCR data presenting transcript levels of IFN-γ, MHC-II, PD-L1, PD-1, Iba-1, CXCL9, CXCL10, and iNOS under the indicated treatment. Data shown are representative of two separate experiments. Supernatants from AI9-stimulated or unstimulated BMNC co-cultured either with microglial cells or astrocytes were collected at 48 h and ELISA was performed for IFN- γ (C), CXCL9 (D), and CXCL10 (E). Blocking of IFN-γ using a neutralizing anti-IFN-γ antibody inhibited CXCL9 (F) and CXCL10 (G) expression. The results shown are from pooled data of two independent experiments. ***$p < 0.001$.

We first assessed the kinetics of MHC-II and PD-L1, which are markers of activation, expression on microglial cells at both 7 and 30 days post prime-CNS boost. Unstimulated microglia, identified as the $CD45^{int}CD11b^{+}$ population using flow cytometry (Figure S3A), have been reported to express minimal levels of MHC-II and PD-L1 (Figures S3B and S3C), whereas a reactive microglial cell phenotype was observed following our prime-CNS boost regimen. Increased expression of MHC-II on microglial cells was first observed during the acute phase (39.5% ± 2.4%) and remained elevated at 30 days post prime-CNS boost (10.5% ± 2.5%), when compared with the control group 5.3% ± 0.4% and 3.2% ± 0.4% at 7 and 30 days, respectively (Figures 6A and 6B). Similarly, expression of PD-L1 was also upregulated at 7 days (30.3% ± 2.6%) and it continued to be expressed at the 30-day time point (17.9% ± 2.2%) (Figures 6C and 6D). PD-L1 expression on microglia was minimal in the control animals (2.8% ± 0.3% and 3.7% ± 0.7% at 7 and 30 days, respectively).

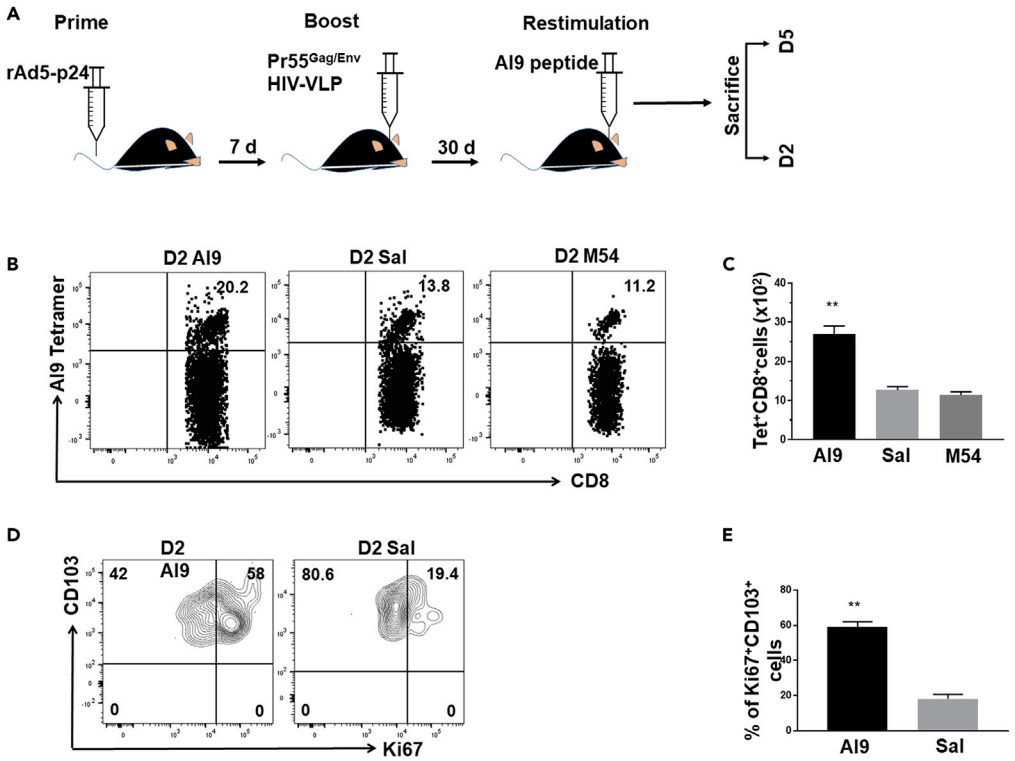

Figure 5. *In Vivo* Recall Responses Stimulate Proliferation of Brain-Resident HIV-Specific CD8$^+$ T Cells

BMNC obtained from prime-CNS boost animals were collected and evaluated using flow cytometry at the indicated time points following *in vivo* peptide restimulation.

(A) Schematic representation of experimental approach to evaluate *in vivo* recall responses. The AI9 peptide, an irrelevant T cell epitope peptide (M54), or saline were injected into the brain and tissues were collected at 2 and 5 days post-restimulation.

(B) Dot plots show tetramer-specific CD8$^+$ T cells in the brain at 2 days post-peptide restimulation.

(C) Bar graph presents numbers of HIV-specific CD8$^+$ T cells following the indicated restimulation.

(D) Contour plots present Ki67 expression on CD103$^+$CD8$^+$ T cells at 2 days post-restimulation with cognate peptide.

(E) Bar graph represents the pooled frequencies of Ki67-expressing CD103$^+$CD8$^+$ T cells. Data are presented as mean ± SD of two independent experiments using four animals in control or irrelevant peptide groups and six animals following AI9 restimulation. **$p < 0.01$

To investigate the effect of recall responses on brain-resident glia, we examined microglial cell activation at 2 and 5 days following restimulation via intracranial injection of AI9 peptide (i.e., at 30 days post prime-CNS boost). We again analyzed MHC-II and PD-L1 expression as microglial activation markers. Interestingly, specific Ag restimulation rapidly induced upregulation of MHC-II expression on microglia cells (74.6% ± 2.9% at 2 days and 49.2% ± 1.6% at 5 days post-restimulation) (Figures 6E and 6B). Similarly, microglia also displayed an increase in PD-L1 (72.4% ± 3.3% at 2 days) that remained elevated (65.1% ± 2.6%) at 5 days following AI9 peptide. Importantly, glial cell activation was not observed in response to MCMV M54 peptide restimulation or saline (Figures 6F and 6D). In addition, i*n vivo* recall immune responses from bT_{RM} may also augment cytotoxic activity within the brain (Figures S4A and S4B).

Reactive Glial Cell Phenotypes in Response to *In Vivo* AI9 Restimulation

We performed IHC on sections of brain obtained from primed-CNS boost mice following 2-day recall stimulation (+AI9), co-staining for MHC-II and Iba-1. Microglial cells within these sections displayed a reactive phenotype, as observed by elevated expression of MHC-II and Iba-1 (Figure 7A). Double immunostaining with anti-TMEM119 (a microglial cell-specific marker) and Iba-1 revealed co-localization following *in vivo* AI9 restimulation (Figure 7A). Expression of CXCL10 was also seen in several locations within the restimulated brain: it was evident in the hippocampus, ventricles, and parenchyma (Figure 7B).

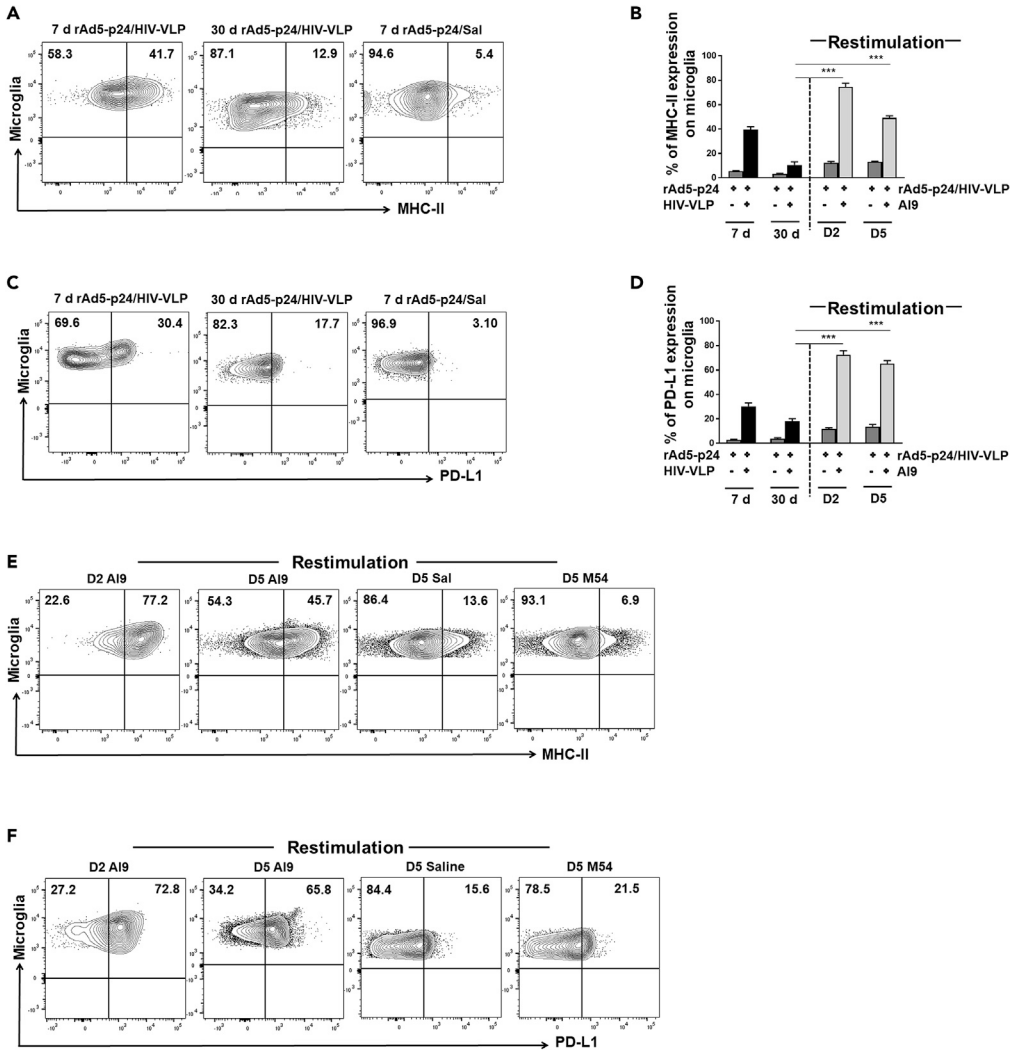

Figure 6. *In Vivo* Recall Responses by bT_{RM} Induce Microglial Cell Activation

Flow cytometry and IHC staining were performed on brain tissue obtained from mice following prime-CNS boost.

(A) Contour plots present expression of MHC-II on $CD45^{int}/CD11b^{+}$ microglia at 7 and 30 days post prime-CNS boost.

(B) Pooled data show the frequencies of MHC-II expression at the indicated time points both pre- and post-recall restimulation via intracranial injection of AI9 peptide.

(C) Contour plots present expression of PD-L1 on stimulated $CD45^{int}/CD11b^{+}$ microglial cells at 7 and 30 days post prime-boost.

(D) Bar graph presented shows frequencies of PD-L1 expression at the indicated time points both pre- and post-restimulation.

(E) Representative contour plots show percentage of microglia expressing MHC-II at 2 and 5 days post *in vivo* AI9 restimulation.

(F) Representative contour plots show the percentage of microglial cells expressing PD-L1 at 2 and 5 days post *in vivo* restimulation. Data presented are mean ± SD of two independent experiments using six animals in control and irrelevant peptide groups at all time points and six to eight animals in the AI9 restimulation group at 7- and 30-day time points, respectively.

***$p < 0.001$.

Most interestingly, dual staining of CXCL10 with Iba-1, as well as the astrocyte marker glial fibrillary acidic protein (GFAP), demonstrated greater co-localization of CXCL10 in the $GFAP^{+}$ population than in the Iba-1^{+} cells (Figure 7C). This finding demonstrated that specific recall responses of bT_{RM} also stimulated astrocytes.

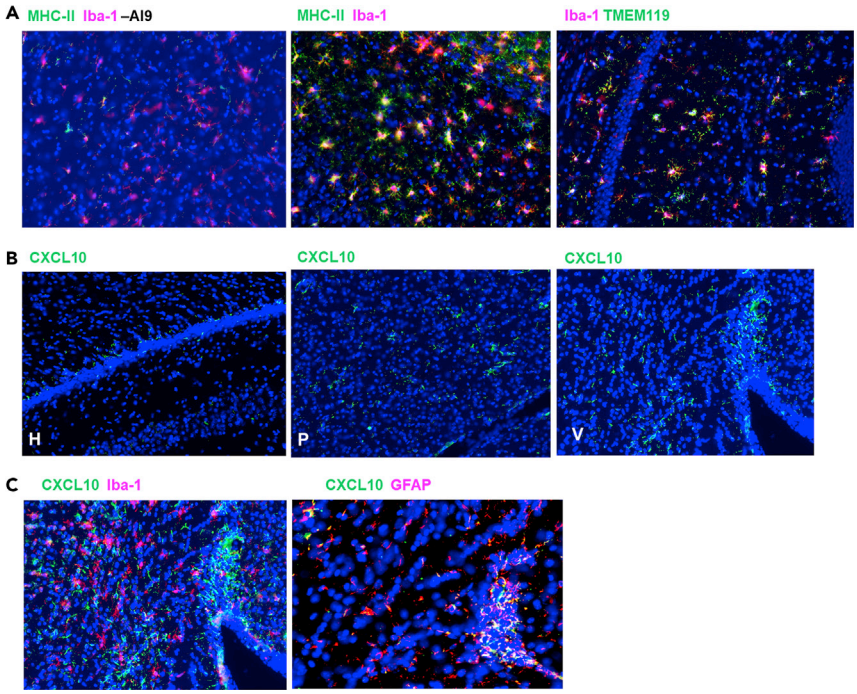

Figure 7. Recall Responses from bTRM Cells Induce Reactive Glial Cell Phenotypes

(A) Dual IHC staining of brain sections obtained from animals at 2 days post-AI9 restimulation for MHC-II and Iba-1, as well as Iba-1 and TMEM119.

(B) IHC staining displaying expression of CXCL10 in the hippocampus (H), parenchyma (P), and ventricle (V) of AI9-restimulated animals.

(C) Images of CXCL10 co-staining with Iba-1, as well as co-expression of CXCL10 and GFAP.

DISCUSSION

During early HIV-1 infection, $CD8^+$ T cell responses play essential roles in viral clearance. As infection proceeds, T_{RM} develop and persist long term in a number of tissues, such as the gastrointestinal tract and female reproductive tract (Kiniry et al., 2018; Tan et al., 2018). These T_{RM} provide robust and immediate effector immune responses to localized reinfection or reactivation of Ag production. The brain is recognized as an important reservoir for latent HIV-1, as well as viral reactivation (Hellmuth et al., 2015). Like other tissues, T_{RM} formation within brain has been demonstrated in several viral infection models (Gebhardt and Mackay, 2012; Prasad et al., 2017; Wakim et al., 2010). It is particularly important to understand recall responses of bT_{RM} because although they appear to be critical in controlling virus, long-term persistent neuroinflammation may lead to deleterious neurocognitive consequences.

Prime-boost regimens have emerged as powerful tools to enhance tissue-infiltrating Ag-specific T cells (Tan et al., 2016, 2018; Zaric et al., 2017). Likewise, the heterologous prime-CNS boost approach used in this study was able to induce brain infiltration of Ag-specific $CD8^+$ T cells. A fraction of these bT_{RM} can be isolated from brain tissue using *ex vivo* dissociation methods. It has been reported that lymphocyte extraction methods fail to efficiently capture all the cells from non-lymphoid tissue and that the efficiency of T_{RM} isolation varies greatly between histologically distinct locations (Steinert et al., 2015). However, the heterologous prime-CNS boost approach used here does provide for the long-term retention of Ag-specific memory cells within the CNS. This observation is in agreement with studies by others wherein Ag-specific $CD8^+$ T cells are preferentially retained in non-lymphoid tissue, even after resolution of infection (Khan et al., 2016; Tan et al., 2016, 2018).

Results presented here demonstrate that long-term retention of HIV-specific $CD8^+$ T cells within brain is coupled with the presence of markers of T_{RM}. High frequencies of $CD8^+CD103^+CD69^+CD49a^+$ were apparent on T cells during the chronic phase following prime-CNS boost. Phenotyping of Ag-specific $CD8^+$ T cells infiltrating the brain revealed distinct populations of SLEC and MPEC from acute into chronic

phases. The KLRG1$^+$ population (i.e., SLEC) dominates at 7 days post prime-CNS boost. In contrast, later time points correlate with development of KLRG1$^-$ CD127$^+$ cells (MPEC). The Ag-specific CD8$^+$ T cells expressed surface CD103, an integrin binding to E-cadherin, and co-expressed CD69 at 30 days. Consistent with other studies, where T_{RMs} in barrier tissues express CD49a and display cytotoxic potential (Cheuk et al., 2017), we found that CD49a was expressed along with other markers of tissue residency; specific peptide stimulation induced granzyme B production (Figures S4A and S4B).

In addition to CD103, CD8$^+$ T_{RM} in non-lymphoid tissue, including human brain, are defined by the CD69 marker (Khan et al., 2016; Smolders et al., 2018). CD69 is an activation marker expressed early that aids in T_{RM} retention by downregulating cell surface expression of S1P1, thereby blocking T cell movement out of tissues (Mackay et al., 2015a; Park and Kupper, 2015). Our findings are similar to those of other studies, where HIV-specific CD8$^+$ T_{RM} were established in murine vaginal mucosa using combined intranasal and intravaginal immunization with recombinant influenza vector (Tan et al., 2018). Generation of long-lived Ag-specific T cell memory has also been demonstrated in mucosal tissue following micro-needle array delivery of adenovirus type 5 vectors encoding HIV-1 Gag (Zaric et al., 2017). Here, we showed that in our prime-CNS boost model, HIV-1-specific CD8$^+$ T cells displayed phenotypic signatures indicative of T_{RM}. Recent studies identify the transcription factors Blimp-1 and homolog of Blimp-1 in T cells (Hobit) in promoting T_{RM} cell development. Blimp and Hobit cooperate to repress genes such as Klf2, S1pr1, and CCR7 (required for tissue egress) and thus contribute to the establishment of tissue residency (Bird, 2016). Similar to these findings, our study demonstrated expression of Blimp-1, along with low levels of T-bet, indicative of long-lived memory cells. Differential expression of these transcription factors in different microenvironments corresponding to varying degrees of inflammation is likely.

T_{RM} survey for their cognate Ag and initiate tissue-wide inflammation to enhance pathogen clearance. T_{RM} that produce abundant IFN-γ and TNF-α, as well as mediators of cytotoxicity, have been identified in a number of infection models (Muruganandah et al., 2018; Prasad et al., 2015; Steinbach et al., 2016). HIV-1-specific CD8$^+$ T_{RM} have been shown to participate in local antiviral immunity (Kiniry et al., 2018). IFN-γ, together with other proinflammatory cytokines, has been shown to induce chemokines and establish chronic immune activation during HIV-1 infection (Roff et al., 2014). In skin, it has been demonstrated that CD49a$^+$ T_{RM} produce IFN-γ and rapidly gain cytotoxic capacity in response to IL-15 (Cheuk et al., 2017). Here, we also demonstrated elevated levels of cytokine production and cytolytic potential of T_{RM} in terms of IFN-γ, IL-2, TNF-α, and granzyme B production. IFN-γ promotes long-term microglial cell activation and TNF- α production (Mutnal et al., 2011). The synergistic action of IFN-γ and TNF- α within the brain has been reported to induce nitric oxide-induced neurodegeneration (Blais and Rivest, 2004). *In vivo* recall immune responses from bT_{RM} may also augment cytotoxic activity within the brain. These findings indicate that potent anti-HIV responses develop upon restimulation with specific T cell epitopes. Our findings are similar to those of other studies wherein robust polyfunctional Gag-specific responses of T_{RM} contribute to HIV-1-specific immunity (Tan et al., 2016, 2018; Zaric et al., 2017).

Although the presence of Ag contributes to bT_{RM} proliferation, the local brain microenvironment also modulates their density and influences their survival. bT_{RM} exhibit limited survival and proliferative capacity *in vitro* (Wakim et al., 2010); however, they do possess self-renewing capacity *in vivo* and display high proliferation during recall responses (Steinbach et al., 2016). Similarly, we found increased proliferation of bT_{RM} upon Ag re-challenge, which suggests retention of their proliferative potential during recall responses. It has also been demonstrated that the density of skin T_{RM} influences local immune protection (Cheuk et al., 2017).

We have previously reported that PD-1 is expressed at high levels on bT_{RM} (Prasad et al., 2017). Yet, despite this upregulation, in the current study bT_{RM} still displayed heightened proliferation and increased cytokine production in response to cognate Ag. This observation further supports the hypothesis that PD-1 is not simply a marker of exhaustion. These findings are in line with those of other studies wherein PD-1$^+$CD8$^+$ T_{RM} displayed transcriptional profiles with effector phenotypes, and showed clonal expansion (Petrelli et al., 2018). PD-1 expression on activated cells is well known to shut down responses to prevent immunopathology (Sharpe et al., 2007). However, in HIV-1 infection it appears that PD-1 expression on bT_{RM} may influence their functional properties in an inflamed brain microenvironment. Therefore, it will be of great interest to further define the roles of PD-1 on bT_{RM} in cART-treated and untreated patients.

T_{RM} are a unique type of memory T cell, specifically tailored to survive in non-lymphoid tissues. However, prolonged bT_{RM}-driven recall responses in a microenvironment that normally lacks routine immune surveillance could be problematic. Persistent neuroimmune activation in response to viral reactivation may result in extensive damage to this largely non-regenerating tissue. Published reports show that a low copy number of HIV-1 provirus can still be intermittently detected in the CSF of patients receiving cART (Spudich et al., 2006; Yilmaz et al., 2006), and persistent CNS inflammation is important to consider during HAND therapy (Saylor et al., 2016). In experimental models, despite low levels of virus, chronically HIV-infected NSG-hCD34$^+$ mice show features of HAND (i.e., brain pathology including activation of microglia, upregulation of neuroinflammatory markers such as Mac1, an indicator of microgliosis, and iNOS), as well as neurodegeneration (Boska et al., 2014; Saylor et al., 2016). In our study, Ag-specific AI9 restimulation *in vivo* showed rapid upregulation of the microglial activation markers MHC-II and PD-L1 at both 2 and 5 days post-restimulation. Furthermore, real-time RT-PCR data from *ex vivo* restimulation experiments demonstrate that recall responses from bT_{RM} are capable of driving microglial cell activation, chemokine production, and production of iNOS. These data demonstrate that glial cells develop reactive phenotypes following the recall response of bT_{RM} to re-challenge with cognate Ag, but not in response to stimulation with non-specific T cell epitopes. Previous studies from our laboratory have identified glial cells as an important source of proinflammatory cytokines and chemokines (Cheeran et al., 2001, 2003; Lokensgard et al., 2016). Reports have shown that the potent T cell chemoattractants CXCL9 and CXCL10 are produced within inflamed brain and that their expression is enhanced by IFN-γ (Lokensgard et al., 2015; Michlmayr and Lim, 2014; Mutnal et al., 2011). Similarly, in this study elevated levels of CXCL9 and CXC10 were observed, expression of which was significantly reduced following blockade of IFN-γ. Production of IFN-γ was found to be specific to the CD8$^+$ T cells as demonstrated by our qPCR data. Following *ex vivo* AI9 restimulation, our data indicate that this cytokine is a driving force for glial cell activation. These findings have implications for neurodegenerative processes by releasing cytotoxic factors such as nitric oxide (NO), as well as several neurotoxic proinflammatory cytokines (Chao et al., 1992; Matsuoka et al., 1999).

Properly regulated neuroimmune responses strike a balance between pathogen clearance and an acceptable level of bystander tissue damage. In cART-treated patients with HAND, there is evidence of lingering, long-term astrocyte activation (Vanzani et al., 2006; Woods et al., 2010). As is the case with microglia, astrocytes also respond to T cell- and microglial cell-produced immune mediators to acquire reactive phenotypes (Liddelow et al., 2017). This cellular activation is routinely visualized by an upregulation of GFAP, a marker of astrogliosis (Burda and Sofroniew, 2014). Here, IHC staining of brain sections from prime-CNS boost mice subjected to recall stimulation further demonstrates the effect of bT_{RM} on glial cell reactivity. Co-localization of MHC-II and Iba-1, as well as GFAP and CXCL10, highlights recall-response-driven reactive phenotypes in both these glial cell types.

In summary, the results reported here demonstrate that our heterologous prime-CNS boost model induces a population of HIV-1-specific bT_{RM}, which persist long term. As viral reactivation from CNS reservoirs appears likely even in cART-experienced patients, this model was used to demonstrate that antiviral recall responses from bT_{RM} can induce tissue-wide reactive gliosis through cytokine-induced activation of brain-resident glia. This cytokine-induced reactive gliosis may protect against viral spread throughout the brain, but it likely has cumulative neurotoxic consequences.

Limitations of the Study

There is no ideal animal model that allows for the invasive study necessary to understand HIV reactivation from brain reservoirs and its association with HAND. It is also unlikely that *in vivo* restimulation with AI9 peptide exactly mimics transient viral protein production within human brain. However, use of this heterologous prime-boost model results in the murine brain being populated by resident memory CD8$^+$ T cells specific for an immunodominant HIV Gag epitope. Subsequent *in vivo* recall neuroimmune responses can then be induced.

METHODS

All methods can be found in the accompanying Transparent Methods supplemental file.

SUPPLEMENTAL INFORMATION

Supplemental Information can be found online at https://doi.org/10.1016/j.isci.2019.10.005.

ACKNOWLEDGMENTS

This project was supported by award numbers NS-038836 from the National Institute of Neurological Disorders and Stroke and MH-066703 from the National Institute of Mental Health.

AUTHOR CONTRIBUTIONS

S.P., S.H., and J.R.L. conceived and designed the experiments. S.P., S.H., W.S.S., and P.C. performed experiments. S.P., S.H., and J.R.L. analyzed the data. S.P. and J.L. wrote the paper. All authors read and approved the final manuscript.

DECLARATION OF INTERESTS

The authors declare no competing interests.

Received: February 1, 2019
Revised: June 26, 2019
Accepted: September 30, 2019
Published: October 25, 2019

REFERENCES

Ariotti, S., Hogenbirk, M.A., Dijkgraaf, F.E., Visser, L.L., Hoekstra, M.E., Song, J.Y., Jacobs, H., Haanen, J.B., and Schumacher, T.N. (2014). T cell memory. Skin-resident memory CD8(+) T cells trigger a state of tissue-wide pathogen alert. Science *346*, 101–105.

Bengsch, B., Spangenberg, H.C., Kersting, N., Neumann-Haefelin, C., Panther, E., von Weizsacker, F., Blum, H.E., Pircher, H., and Thimme, R. (2007). Analysis of CD127 and KLRG1 expression on hepatitis C virus-specific CD8+ T cells reveals the existence of different memory T-cell subsets in the peripheral blood and liver. J. Virol. *81*, 945–953.

Bird, L. (2016). Lymphocyte responses: Hunker down with HOBIT and BLIMP1. Nat. Rev. Immunol. *16*, 338–339.

Blais, V., and Rivest, S. (2004). Effects of TNF-alpha and IFN-gamma on nitric oxide-induced neurotoxicity in the mouse brain. J. Immunol. *172*, 7043–7052.

Boska, M.D., Dash, P.K., Knibbe, J., Epstein, A.A., Akhter, S.P., Fields, N., High, R., Makarov, E., Bonasera, S., Gelbard, H.A., et al. (2014). Associations between brain microstructures, metabolites, and cognitive deficits during chronic HIV-1 infection of humanized mice. Mol. Neurodegener. *9*, 58.

Burda, J.E., and Sofroniew, M.V. (2014). Reactive gliosis and the multicellular response to CNS damage and disease. Neuron *81*, 229–248.

Chao, C.C., Hu, S., Molitor, T.W., Shaskan, E.G., and Peterson, P.K. (1992). Activated microglia mediate neuronal cell injury via a nitric oxide mechanism. J. Immunol. *149*, 2736–2741.

Cheeran, M.C., Hu, S., Yager, S.L., Gekker, G., Peterson, P.K., and Lokensgard, J.R. (2001). Cytomegalovirus induces cytokine and chemokine production differentially in microglia and astrocytes: antiviral implications. J. Neurovirol. *7*, 135–147.

Cheeran, M.C., Hu, S., Sheng, W.S., Peterson, P.K., and Lokensgard, J.R. (2003). CXCL10 production from cytomegalovirus-stimulated microglia is regulated by both human and viral interleukin-10. J. Virol. *77*, 4502–4515.

Chen, M.F., Gill, A.J., and Kolson, D.L. (2014). Neuropathogenesis of HIV-associated neurocognitive disorders: roles for immune activation, HIV blipping and viral tropism. Curr. Opin. HIV AIDS *9*, 559–564.

Cheuk, S., Schlums, H., Gallais Serezal, I., Martini, E., Chiang, S.C., Marquardt, N., Gibbs, A., Detlofsson, E., Introini, A., Forkel, M., et al. (2017). CD49a expression defines tissue-resident CD8(+) T cells poised for cytotoxic function in human skin. Immunity *46*, 287–300.

Childers, M.E., Woods, S.P., Letendre, S., McCutchan, J.A., Rosario, D., Grant, I., Mindt, M.R., and Ellis, R.J.; San Diego HIV Neurobehavioral Research Center Group (2008). Cognitive functioning during highly active antiretroviral therapy interruption in human immunodeficiency virus type 1 infection. J. Neurovirol. *14*, 550–557.

Ganesh, A., Lemongello, D., Lee, E., Peterson, J., McLaughlin, B.E., Ferre, A.L., Gillespie, G.M., Fuchs, D., Deeks, S.G., Hunt, P.W., et al. (2016). Immune activation and HIV-specific CD8(+) T cells in cerebrospinal fluid of HIV controllers and noncontrollers. AIDS Res. Hum. Retroviruses *32*, 791–800.

Gebhardt, T., and Mackay, L.K. (2012). Local immunity by tissue-resident CD8(+) memory T cells. Front. Immunol. *3*, 340.

Gisslen, M., Rosengren, L., Hagberg, L., Deeks, S.G., and Price, R.W. (2005). Cerebrospinal fluid signs of neuronal damage after antiretroviral treatment interruption in HIV-1 infection. AIDS Res. Ther. *2*, 6.

Graham, D.R., Gama, L., Queen, S.E., Li, M., Brice, A.K., Kelly, K.M., Mankowski, J.L., Clements, J.E., and Zink, M.C. (2011). Initiation of HAART during acute simian immunodeficiency virus infection rapidly controls virus replication in the CNS by enhancing immune activity and preserving protective immune responses. J. Neurovirol. *17*, 120–130.

Grauer, O.M., Reichelt, D., Gruneberg, U., Lohmann, H., Schneider-Hohendorf, T., Schulte-Mecklenbeck, A., Gross, C.C., Meuth, S.G., Wiendl, H., and Husstedt, I.W. (2015). Neurocognitive decline in HIV patients is associated with ongoing T-cell activation in the cerebrospinal fluid. Ann. Clin. Transl. Neurol. *2*, 906–919.

Hellmuth, J., Valcour, V., and Spudich, S. (2015). CNS reservoirs for HIV: implications for eradication. J. Virus Erad. *1*, 67–71.

Ho, E.L., Ronquillo, R., Altmeppen, H., Spudich, S.S., Price, R.W., and Sinclair, E. (2013). Cellular composition of cerebrospinal fluid in HIV-1 infected and uninfected subjects. PLoS One *8*, e66188.

Kaech, S.M., and Wherry, E.J. (2007). Heterogeneity and cell-fate decisions in effector and memory CD8+ T cell differentiation during viral infection. Immunity *27*, 393–405.

Khan, T.N., Mooster, J.L., Kilgore, A.M., Osborn, J.F., and Nolz, J.C. (2016). Local antigen in nonlymphoid tissue promotes resident memory CD8+ T cell formation during viral infection. J. Exp. Med. *213*, 951–966.

Kiniry, B.E., Li, S., Ganesh, A., Hunt, P.W., Somsouk, M., Skinner, P.J., Deeks, S.G., and Shacklett, B.L. (2018). Detection of HIV-1-specific gastrointestinal tissue resident CD8(+) T-cells in chronic infection. Mucosal Immunol. *11*, 909–920.

Kowarik, M.C., Grummel, V., Wemlinger, S., Buck, D., Weber, M.S., Berthele, A., and Hemmer, B. (2014). Immune cell subtyping in the cerebrospinal fluid of patients with neurological diseases. J. Neurol. *261*, 130–143.

Lamers, S.L., Rose, R., Ndhlovu, L.C., Nolan, D.J., Salemi, M., Maidji, E., Stoddart, C.A., and McGrath, M.S. (2016). The meningeal lymphatic system: a route for HIV brain migration? J. Neurovirol. *22*, 275–281.

Liddelow, S.A., Guttenplan, K.A., Clarke, L.E., Bennett, F.C., Bohlen, C.J., Schirmer, L., Bennett, M.L., Munch, A.E., Chung, W.S., Peterson, T.C., et al. (2017). Neurotoxic reactive astrocytes are induced by activated microglia. Nature *541*, 481–487.

Lokensgard, J.R., Schachtele, S.J., Mutnal, M.B., Sheng, W.S., Prasad, S., and Hu, S. (2015). Chronic reactive gliosis following regulatory T cell depletion during acute MCMV encephalitis. Glia *63*, 1982–1996.

Lokensgard, J.R., Mutnal, M.B., Prasad, S., Sheng, W., and Hu, S. (2016). Glial cell activation, recruitment, and survival of B-lineage cells following MCMV brain infection. J. Neuroinflammation *13*, 114.

Mackay, L.K., Rahimpour, A., Ma, J.Z., Collins, N., Stock, A.T., Hafon, M.L., Vega-Ramos, J., Lauzurica, P., Mueller, S.N., Stefanovic, T., et al. (2013). The developmental pathway for CD103(+) CD8+ tissue-resident memory T cells of skin. Nat. Immunol. *14*, 1294–1301.

Mackay, L.K., Braun, A., Macleod, B.L., Collins, N., Tebartz, C., Bedoui, S., Carbone, F.R., and Gebhardt, T. (2015a). Cutting edge: CD69 interference with sphingosine-1-phosphate receptor function regulates peripheral T cell retention. J. Immunol. *194*, 2059–2063.

Mackay, L.K., Wynne-Jones, E., Freestone, D., Pellicci, D.G., Mielke, L.A., Newman, D.M., Braun, A., Masson, F., Kallies, A., Belz, G.T., et al. (2015b). T-box transcription factors combine with the cytokines TGF-beta and IL-15 to control tissue-resident memory T cell fate. Immunity *43*, 1101–1111.

Marcondes, M.C., Burdo, T.H., Sopper, S., Huitron-Resendiz, S., Lanigan, C., Watry, D., Flynn, C., Zandonatti, M., and Fox, H.S. (2007). Enrichment and persistence of virus-specific CTL in the brain of simian immunodeficiency virus-infected monkeys is associated with a unique cytokine environment. J. Immunol. *178*, 5812–5819.

Masopust, D., Vezys, V., Wherry, E.J., Barber, D.L., and Ahmed, R. (2006). Cutting edge: gut microenvironment promotes differentiation of a unique memory CD8 T cell population. J. Immunol. *176*, 2079–2083.

Masopust, D., Choo, D., Vezys, V., Wherry, E.J., Duraiswamy, J., Akondy, R., Wang, J., Casey, K.A., Barber, D.L., Kawamura, K.S., et al. (2010). Dynamic T cell migration program provides resident memory within intestinal epithelium. J. Exp. Med. *207*, 553–564.

Matsuoka, Y., Kitamura, Y., Takahashi, H., Tooyama, I., Kimura, H., Gebicke-Haerter, P.J., Nomura, Y., and Taniguchi, T. (1999). Interferon-gamma plus lipopolysaccharide induction of delayed neuronal apoptosis in rat hippocampus. Neurochem. Int. *34*, 91–99.

McMaster, S.R., Wilson, J.J., Wang, H., and Kohlmeier, J.E. (2015). Airway-resident memory CD8 T cells provide antigen-specific protection against respiratory virus challenge through rapid IFN-gamma production. J. Immunol. *195*, 203–209.

Michlmayr, D., and Lim, J.K. (2014). Chemokine receptors as important regulators of pathogenesis during arboviral encephalitis. Front. Cell. Neurosci. *8*, 264.

Monteiro de Almeida, S., Letendre, S., Zimmerman, J., Lazzaretto, D., McCutchan, A., and Ellis, R. (2005). Dynamics of monocyte chemoattractant protein type one (MCP-1) and HIV viral load in human cerebrospinal fluid and plasma. J. Neuroimmunol. *169*, 144–152.

Mueller, S.N., and Mackay, L.K. (2016). Tissue-resident memory T cells: local specialists in immune defence. Nat. Rev. Immunol. *16*, 79–89.

Muruganandah, V., Sathkumara, H.D., Navarro, S., and Kupz, A. (2018). A systematic review: the role of resident memory T cells in infectious diseases and their relevance for vaccine development. Front. Immunol. *9*, 1574.

Mutnal, M.B., Hu, S., Little, M.R., and Lokensgard, J.R. (2011). Memory T cells persisting in the brain following MCMV infection induce long-term microglial activation via interferon-gamma. J. Neurovirol. *17*, 424–437.

Park, C.O., and Kupper, T.S. (2015). The emerging role of resident memory T cells in protective immunity and inflammatory disease. Nat. Med. *21*, 688–697.

Petrelli, A., Mijnheer, G., Hoytema van Konijnenburg, D.P., van der Wal, M.M., Giovannone, B., Mocholi, E., Vazirpanah, N., Broen, J.C., Hijnen, D., Oldenburg, B., et al. (2018). PD-1+CD8+ T cells are clonally expanding effectors in human chronic inflammation. J. Clin. Invest. *128*, 4669–4681.

Prasad, S., Hu, S., Sheng, W.S., Singh, A., and Lokensgard, J.R. (2015). Tregs modulate lymphocyte proliferation, activation, and resident-memory T-cell accumulation within the brain during MCMV infection. PLoS One *10*, e0145457.

Prasad, S., Hu, S., Sheng, W.S., Chauhan, P., Singh, A., and Lokensgard, J.R. (2017). The PD-1: PD-L1 pathway promotes development of brain-resident memory T cells following acute viral encephalitis. J. Neuroinflammation *14*, 82.

Roff, S.R., Noon-Song, E.N., and Yamamoto, J.K. (2014). The significance of interferon-gamma in HIV-1 pathogenesis, therapy, and prophylaxis. Front. Immunol. *4*, 498.

Saylor, D., Dickens, A.M., Sacktor, N., Haughey, N., Slusher, B., Pletnikov, M., Mankowski, J.L., Brown, A., Volsky, D.J., and McArthur, J.C. (2016). HIV-associated neurocognitive disorder–pathogenesis and prospects for treatment. Nat. Rev. Neurol. *12*, 234–248.

Schenkel, J.M., and Masopust, D. (2014). Tissue-resident memory T cells. Immunity *41*, 886–897.

Schrier, R.D., Hong, S., Crescini, M., Ellis, R., Perez-Santiago, J., Spina, C., Letendre, S., and Group, H. (2015). Cerebrospinal fluid (CSF) CD8+ T-cells that express interferon-gamma contribute to HIV associated neurocognitive disorders (HAND). PLoS One *10*, e0116526.

Sharpe, A.H., Wherry, E.J., Ahmed, R., and Freeman, G.J. (2007). The function of programmed cell death 1 and its ligands in regulating autoimmunity and infection. Nat. Immunol. *8*, 239–245.

Slutter, B., Pewe, L.L., Kaech, S.M., and Harty, J.T. (2013). Lung airway-surveilling CXCR3(hi) memory CD8(+) T cells are critical for protection against influenza A virus. Immunity *39*, 939–948.

Smolders, J., Heutinck, K.M., Fransen, N.L., Remmerswaal, E.B.M., Hombrink, P., Ten Berge, I.J.M., van Lier, R.A.W., Huitinga, I., and Hamann, J. (2018). Tissue-resident memory T cells populate the human brain. Nat. Commun. *9*, 4593.

Spudich, S., Lollo, N., Liegler, T., Deeks, S.G., and Price, R.W. (2006). Treatment benefit on cerebrospinal fluid HIV-1 levels in the setting of systemic virological suppression and failure. J. Infect. Dis. *194*, 1686–1696.

Stam, A.J., Nijhuis, M., van den Bergh, W.M., and Wensing, A.M. (2013). Differential genotypic evolution of HIV-1 quasispecies in cerebrospinal fluid and plasma: a systematic review. AIDS Rev. *15*, 152–161.

Steinbach, K., Vincenti, I., Kreutzfeldt, M., Page, N., Muschaweckh, A., Wagner, I., Drexler, I., Pinschewer, D., Korn, T., and Merkler, D. (2016). Brain-resident memory T cells represent an autonomous cytotoxic barrier to viral infection. J. Exp. Med. *213*, 1571–1587.

Steinert, E.M., Schenkel, J.M., Fraser, K.A., Beura, L.K., Manlove, L.S., Igyarto, B.Z., Southern, P.J., and Masopust, D. (2015). Quantifying memory CD8 T cells reveals regionalization of immunosurveillance. Cell *161*, 737–749.

Tan, H.X., Gilbertson, B.P., Jegaskanda, S., Alcantara, S., Amarasena, T., Stambas, J., McAuley, J.L., Kent, S.J., and De Rose, R. (2016). Recombinant influenza virus expressing HIV-1 p24 capsid protein induces mucosal HIV-specific CD8 T-cell responses. Vaccine *34*, 1172–1179.

Tan, H.X., Wheatley, A.K., Esterbauer, R., Jegaskanda, S., Glass, J.J., Masopust, D., De Rose, R., and Kent, S.J. (2018). Induction of vaginal-resident HIV-specific CD8 T cells with mucosal prime-boost immunization. Mucosal Immunol. *11*, 994–1007.

Vanzani, M.C., Iacono, R.F., Caccuri, R.L., Troncoso, A.R., and Berria, M.I. (2006). Regional differences in astrocyte activation in HIV-associated dementia. Medicina (B Aires) *66*, 108–112.

Wakim, L.M., Woodward-Davis, A., and Bevan, M.J. (2010). Memory T cells persisting within the brain after local infection show functional adaptations to their tissue of residence. Proc. Natl. Acad. Sci. U S A *107*, 17872–17879.

Watanabe, R., Gehad, A., Yang, C., Scott, L.L., Teague, J.E., Schlapbach, C., Elco, C.P., Huang, V., Matos, T.R., Kupper, T.S., et al. (2015). Human skin is protected by four functionally and phenotypically discrete populations of resident and recirculating memory T cells. Sci. Transl. Med. *7*, 279ra239.

Woods, S.P., Iudicello, J.E., Dawson, M.S., Weber, E., Grant, I., and Letendre, S.L.; HIV Neurobehavioral Research Center (HNRC) Group (2010). HIV-associated deficits in action (verb) generation may reflect astrocytosis. J. Clin. Exp. Neuropsychol. *32*, 522–527.

Woon, H.G., Braun, A., Li, J., Smith, C., Edwards, J., Sierro, F., Feng, C.G., Khanna, R., Elliot, M., Bell, A., et al. (2016). Compartmentalization of total and virus-specific tissue-resident memory CD8+ T cells in human lymphoid organs. PLoS Pathog. *12*, e1005799.

Yilmaz, A., Fuchs, D., Hagberg, L., Nillroth, U., Stahle, L., Svensson, J.O., and Gisslen, M. (2006). Cerebrospinal fluid HIV-1 RNA, intrathecal immunoactivation, and drug concentrations after treatment with a combination of saquinavir, nelfinavir, and two nucleoside analogues: the M61022 study. BMC Infect. Dis. *6*, 63.

Yuzefpolskiy, Y., Baumann, F.M., Kalia, V., and Sarkar, S. (2015). Early CD8 T-cell memory precursors and terminal effectors exhibit equipotent in vivo degranulation. Cell. Mol. Immunol. *12*, 400–408.

Zaric, M., Becker, P.D., Hervouet, C., Kalcheva, P., Ibarzo Yus, B., Cocita, C., O'Neill, L.A., Kwon, S.Y., and Klavinskis, L.S. (2017). Long-lived tissue resident HIV-1 specific memory CD8(+) T cells are generated by skin immunization with live virus vectored microneedle arrays. J. Control. Release *268*, 166–175.

ISCI, Volume *20*

Supplemental Information

Recall Responses from Brain-Resident Memory CD8$^+$ T Cells (bT_{RM}) Induce Reactive Gliosis

Sujata Prasad, Shuxian Hu, Wen S. Sheng, Priyanka Chauhan, and James R. Lokensgard

Transparent Methods

METHODS

Ethical statement

This study was carried out in strict accordance with recommendations in the Guide for the Care and Use of Laboratory Animals of the National Institutes of Health. The protocol was approved by the Institutional Animal Care and Use Committee (Protocol Number: 1701-34513A) of the University of Minnesota. All surgery was performed under Ketamine/Xylazine anesthesia and all efforts were made to minimize suffering.

Virus and animals

Six to eight week old BALB/c mice were vaccinated via tail-vein injection with an adenovirus vector (1 x 10^{10} PFU/mouse) expressing the HIV-1 p24 capsid protein (rAd5-p24). We outsourced production of a 2nd-generation (i.e., ΔE1 + ΔE3), replication incompetent adenovirus vector to Cyagen Biosciences (Santa Clara, CA), which expresses the HIV-1 capsid protein p24 under control of the minimal CMV IE promoter (i.e., rAd5-p24). Following vaccination, to promote immune cell infiltration and retention in the brain, animals were then boosted (7d later) via an intracranial injection of HIV virus-like particles (HIV-VLPs). Animals received 300 fluorescent units (FU) of HIVLP in a volume no greater than 5ul delivered to the brain striatum via stereotaxic injection.

Production of HIV virus-like particles (HIV-VLPs)

HIV-VLPs were produced by transfection of HEK 293T cells with pEYFP-N3 HIV-1, a Gag-expressing codon-optimized plasmid encoding the 55kDa Gag precursor protein fused to enhanced yellow fluorescent protein (EYFP), under control of the human CMV IE promoter, obtained from Louis Mansky (Institute for Molecular Virology, University of Minnesota); p3NL(ADA)env,

encoding a full length R5-tropic envelope protein, under control of the HIV-1 LTR promoter, was obtained with permission from Eric Freed (NCI, Frederick, MD). To produce Gag-alone HIV-VLPs, cells are transfected with only Gag plasmid. 293T cells were co-transfected with Gag, pCEP4-Tat, and Env plasmid. Because these HIV-VLPs express EYFP, fluorescent units (FU) were used as an indicator of quantity. ELISA was also used to determine the concentrations of Gag protein in individual HIV-VLP batches using a p24 Ag capture assay. Ratios of gp120 to EYFP for a given batch were calculated to ensure similar quantities were administered per dose. An HIV-VLP dose of 300 FU equivalents conferred reliable stimulation and promoted peripheral immune cell infiltration into the brain.

Intracranial injection of mice

Injection of mice was performed as previously described with slight modifications (Cheeran et al., 2004). Briefly, female mice (6–8 week old) were anesthetized using a combination of Ketamine (Akorn, Inc. Lake Forest, IL) and Xylazine (Bimeda Inc., Le Sueur, MN), (100 mg and 10 mg/kg body weight, respectively) and immobilized on a small animal stereotactic instrument equipped with a Cunningham mouse adapter (Stoelting Co., Wood Dale, IL). Subcutaneous injection of the analgesic bupivacaine (Hospira, Inc. Lake Forest, IL), (1-2 mg/kg [0.4-0.8 ml/kg of a 0.25% solution]) in the area prior to incision was performed to minimize pain. The skin and underlying connective tissue were reflected to expose reference sutures (sagittal and coronal) on the skull. The sagittal plane was adjusted such that bregma and lambda were positioned at the same coordinates on the vertical plane. A burr hole was drilled to expose the underlying dura at pre-determined coordinates to access the left striatum (AP = 0 mm, ML = 2.0 mm from bregma, and DV = 3.0 from skull surface). Animals received 300 FU of HIV-VLP in a volume no greater than 5 µl delivered to striatum via stereotaxic injection, using a Hamilton syringe (10 µl) fitted to a 27 G

needle. The injection was delivered over a period of 5 min. The needle was retracted slowly and burr hole was closed with sterile bone-wax, the animal was removed from the stereotaxic apparatus and the skin incision was closed with 4-0 silk sutures with a FS-2 needle (Ethicon, Somerville NJ).

Ag Restimulation

Restimulation with HIV-1-specific T-cell epitope peptide was performed 30 d post HIV-VLP. Previous studies have identified the capsid p24 H-2K^{d} MHC class I-restricted peptide AMQMLKETI (i.e., AI9) as an immunodominant epitope (Tan et al., 2016; Tan et al., 2018). Animals were injected with 100 μM AI9 peptide in 5-μl saline delivered into the brain striatum. Brain tissue was isolated at 2 and 5 d post-restimulation. BMNC were examined for Ag-specific CD8^{+} T-cells, as well as microglial cell activation, by flow cytometry, whereas brain tissue sections were collected at 2 d for IHC staining and qPCR.

Brain leukocyte isolation and flow cytometry analysis

BMNC were isolated from the brain of prime-CNS boost animals using a previously described procedure with minor modifications (Cheeran et al., 2007; Ford et al., 1995; Marten et al., 2003; Mutnal et al., 2011). In brief, whole brain tissues were harvested (n = 4-6 animals/group/experiment), and minced finely using a scalpel in RPMI 1640 (2 g/L D-glucose and 10 mM HEPES) and digested in 0.0625% trypsin (in Ca/Mg-free HBSS) at room temperature for 20 min. Single cell preparations of infected brains were resuspended in 30% Percoll (Sigma-Aldrich, St. Louis, MO) and banded on a 70% Percoll cushion at 900 × g for 30 min at 15°C. Brain leukocytes obtained from the 30–70% Percoll interface were collected. Following preparation of single cell suspensions, cells were treated with Fc block (anti-CD32/CD16 in the form of 2.4G2 hybridoma culture supernatant with 2% normal rat and 2% normal mouse serum) to inhibit nonspecific Ab binding. Cells were then counted using the trypan blue dye exclusion method, and

1 x 10^6 cells were subsequently stained with anti-mouse immune cell surface markers for 15-20 min at 4°C (anti-CD45-BV605, anti-KLRG1-PE-Cy7, anti-CD11b-AF700, anti-CD103-FITC, anti-CD127-PECy-5, anti-CD69-e-F 450, anti-CD49a-PE, anti-PD1-BV711 (Previously eBioscience, Thermo Fisher Scientific, Waltham, MA) and anti-CD8-BV-510 (clone YTS156.7.7) from (Biolegend, San Diego, CA). Control isotype Abs were used for all fluorochrome combinations to assess nonspecific Ab binding. For tetramer staining, the H-2K^d major histocompatibility complex (MHC) class I-restricted peptide AMQMLKETI (AI9) as the immunodominant T-cell epitope was purchased from MBL Corporation (Woburn, MA) and used for evaluation of Ag-specific responses. 200,000 events were recorded and live leukocytes were gated using forward scatter and side scatter parameters on a LSRII H4760 (BD Biosciences, San Jose CA). The gating strategy is shown in Supplementary Figures (S1B, C and D). Data were analyzed using FlowJo software (FlowJo, Ashland, OR).

Intracellular cytokine staining

To assess intracellular cytokine production, BMNC (2 x 10^6 cells/well) were incubated either with polyclonal stimulation using anti-CD3/CD28 or HIV-1-specific peptide for 5h at 37°C in RPMI complete medium supplemented with 10% FBS. Brefeldin A (1 µl/ml) was present throughout the incubation. Peptide was omitted in negative control samples. Cells were surface stained prior to fixation/permeabilization using cytofix/cytosperm kit (Thermo Fisher Scientific). Cells were then stained for Ki67-PE, IFN-γ, eF450, IL-2-PE-cy7, TNF-α-APC (Thermo Fisher Scientific) and Granzyme B-APC (Biolegend). Transcription factors associated with T_{RM} development like Blimp-1(Biolegend), Eomes (Invitrogen, Carlsbad, CA), and T-bet (Thermo Fisher Scientific) were stained, as recommended by manufacturer's protocol. Stained cells were analyzed as described above.

Real-time RT-PCR

Cultures of BMNC with or without $CD8^+$ T-cells (depleted through positive isolation using a Miltenyi Biotech Kit (Bergisch Gladbach, Germany) from post prime-CNS boost animals at 30 d were used. BMNC were either stimulated with AI9 peptide or left unstimulated for 1h before being co-cultured with mixed glial cells (40% microglia; 60% astrocytes) for 24 h. $CD8^+$ T-cells were added at 10:1 CD8: glial cell ratio. RNA was extracted from co-cultured cells using the RNeasy® Lipid Tissue Mini kit (Qiagen, Valencia, CA), treated with DNase and reverse transcribed to cDNA with oligo $(dT)_{12–18}$, random hexmer, dNTPs (Gene Link, Hawthorne, NY), RNase inhibitor and SuperScript™ III reverse transcriptase (Invitrogen). Diluted cDNA, primers and SYBR® Advantage® qPCR premix (ClonTech, now Takara Bio USA, Mountain View, CA) were subjected to real-time PCR (Bio-Rad Laboratories, Hercules, CA) according to the manufacturer's protocol. Primer sequences were: sense 5'-GCGTCATTGAATCACACCTG-3' and antisense 5'- GACCTGTGGGTTGTTGACCT-3' for IFN-γ (104 bp); sense 5'-GACGCTCAACTTGTCCCAAAAC -3' and antisense 5'- GCAGCCGTGAACTTGTTGAAC -3' for MHC-II (200 bp); sense 5'- CGTGAGTGGGAAGAGAAGTGTC-3' and antisense 5'-CTACAATGAGGAACAACAGGATGG-3' for PD-L1 (239 bp); sense 5'GACTTCCACATGAACATCCTTGAC-3' and antisense 5'CTCTGGCCTCTGACATACTTGTTG-3' for PD-1 (295 bp); sense 5'-GTCATTTTCTGCCTCATCCTGCT-3' and antisense 5'-GGATTCAGACATCTCTGCTCATCA-3' for CXCL10 (212 bp); sense 5'-AGAACGGAGATCAAACCTGCCT-3' and antisense 5'- CGACTTTGGGGTGTTTTGGGTT-3' for CXCL9 (157 bp); sense 5'- GGAGGGGATCAACAAGCAATTCCT-3' and antisense 5'-GGAGCCACTGGACACCTCTCTAAT-3' for Iba-1 (220 bp) sense 5'-

TGGCCACCTTGTTCAGCTACG-3' and antisense 5'- GCCAAGGCCAAACACAGCATA-3' for iNOS (212 bp); and sense 5'- TGCTCGAGATGTCATGAAGG-3' and antisense 5'- AATCCAGCAGGTCAGCAAAG-3' for HPRT (hypoxanthine phosphoribosyltransferase, 95 bp). The PCR conditions for the Bio-Rad CFX96 qPCR System were: 1 denaturation cycle at 95°C for 10 s; 40 amplification cycles of 95°C for 10 s, 60°C annealing for 10 s, and elongation at 72°C for 10 s; followed by 1 dissociation cycle. The relative product levels were quantified using the $2^{-\Delta\Delta Ct}$ method (Livak and Schmittgen, 2001) and were normalized to the housekeeping gene HPRT.

Primary glial cell cultures

Cerebral cortical cells from 1 d old Balb/c mice were dissociated after a 30 min trypsinization (0.25 %) in HBSS and plated in 75 cm2 culture flasks in DMEM containing 6 % FBS, penicillin (100 U/ml), streptomycin (100 µg/ml), gentamicin (50 µg/ml), and Fungizone® amphotericin B (250 pg/ml). The medium was replenished 1 and 4 d after plating. On 12 d of culture, floating microglial cells were harvested and plated onto 48-well cell culture plates (1×10^5 cells/well). After a 1 h incubation at 37 °C, the culture plates were washed and incubated overnight before starting the experiments. Purified microglial cell cultures were comprised of a cell population in which >95 % stained positively with Iba-1 antibodies and 3–5 % stained positively with antibodies specific to GFAP. Purified astrocyte cultures were prepared from the culture flask following isolation of microglia at 14 days *in vitro*. Briefly, after collection of microglia, the culture flasks were shaken at 180–200 rpm at 37 °C for 16 h followed by trypsinization (0.25 % trypsin in HBSS) for 30 min. Cells were seeded into new flasks with DMEM, after adding FBS (final concentration 10 %), centrifugation, and washing. The medium was changed after 24 h. This subculture procedure was repeated weekly for 2–3 times to remove residual oligodendrocytes and microglia,

in order to achieve highly purified astrocyte cultures (95–98 % of cells reacted with GFAP Ab, 3-5 % stained with Iba-1 Ab), which were plated onto 48-well culture plates (1×10^5 cells/well).

ELISA

The supernatants from AI9-stimulated BMNC (30 d post-prime-CNS boost) co-cultured either with purified microglial cells or astrocytes (48 h) were collected for ELISA. In brief, 96-well ELISA plates were pre-coated with anti-mouse CXCL9, CXCL10 (R&D Minneapolis, MN), or IFN-γ (Invitrogen) Abs (2 μg/ml) overnight at 4 °C and blocked with 1 % BSA in PBS for 1 h at room temperature (RT). After washing (PBS with Tween 20), supernatants and a series of diluted standards were added to the wells for 2 h at RT. Abs to anti-CXCL9, CXCL10 and IFN-γ were added and incubated for 90 min at RT followed by addition of secondary Abs conjugated with horseradish peroxidase (according to manufacturer's guidelines) for 45 min at RT. The chromogen substrate K-Blue (Neogen, Lexington, KY) was added for color development, which was terminated with 1 M H_2SO_4. The plates were read at 450 nm, and concentration levels of cytokine and chemokines were extrapolated from standard curves, normalized to protein concentrations.

Immunohistochemistry

Brains were harvested from prime-CNS boost mice with or without AI9 restimulation for 2 d. Animals were perfused with serial washes of 2% sodium nitrate and phosphate-buffered saline (PBS) to remove contaminating blood cells, and prefixed with 4% paraformaldehyde. Murine brains were subsequently submerged in 4% paraformaldehyde for 24 h and transferred to 25% sucrose solution for 2 d prior to sectioning. After blocking (PBS with 10% normal donkey serum and 0.3% Triton X-100) for 1 h at RT, brain sections (25 μm) were incubated overnight at 4°C with the following primary antibodies: Rat anti-mouse MHC-II (10 μg/mL; eBioscience, San Diego CA), Goat anti-mouse CXCL10 (10μg/mL; R&D Systems, Minneapolis, MN) , Rabbit anti

GFAP (1:500; DAKO, Sunnyvale, CA), Rabbit anti Iba-1 (2ug/ml; Wako chemicals, Richmond, VA) and Rabbit anti-TMEM119 antibody (Abcam, Cambridge, MA). Brain sections were washed four times with PBS. After washing, secondary antibody (Donkey anti Rat FITC-conjugate, Donkey anti Goat NL577-conjugate and Donkey anti NL493-conjugate was added for 1h at RT followed by nuclear labeling with Hoechst 33342 (1 μg/ml; Chemicon, Temecula, CA) and viewed under a fluorescent microscope.

Statistical analysis

For comparing groups, a two-tailed unpaired Student's T-test for samples was applied, p values $\leq$ 0.05 were considered significant.

Supplemental information

Figure S1: Expression of HIV-p24 in murine liver (related to Figure 1). A. IHC staining of murine liver sections for HIV-1 p24 protein 7 d post-priming via intravenous injection with rAd5-p24 (1 x 10^{10} PFU) confirms that the construct delivers bona fide p24 protein which is expressed *in vivo*. **B.** Flow cytometry gating strategy for the rAd5-p24/Sal group. **C.** Flow cytometry gating strategy for the rAd5-p24/ HIV-VLP group. **D.** Quantification of tetramer signaling on non-$CD8^+$ T-cells at 7 d and 30 d post-prime CNS boost**.**

Figure S2: Frequency of $CD4^+$ and $CD8^+$ T-cells (related to Figure 1 & Figure 4). A. Frequency of $CD4^+$ and $CD8^+$ T-cells at the indicated time points among rAd5-p24/ HIV-VLP animals. **B.** Representative plot showing successful depletion of $CD8^+$ T-cells isolated from the

brain of post prime-CNS boost animals using the Miltenyi Biotech Kit (Bergisch Gladbach Germany).

Figure S3: Gating strategy for microglial cells (related to Figure 6). A. Microglia were identified as the $CD45^{int}CD11b^{+}$ population within total BMNC. **B.** Representative images of microglial cell populations showing expression of the activation marker MHC-II in respective control groups. **C.** Contour plots show expression of the microglial activation marker PD-L1 in the indicated groups (i.e., treatment with either rAd5-p24, HIV-VLP, or rAd5-p24/Sal).

Figure S4: Cytotoxic potential of $CD103^{+}CD8^{+}$ bT_{RM} following AI9 restimulation (related to Figure 1 & Figure 6). BMNC were obtained from heterologous prime-boost animals at 2 & 5 d post-AI9 restimulation *in vivo* and intracellular staining was performed. **A.** Representative contour plots display granzyme B production by $CD103^{+}CD8^{+}$ T-cells in response to AI9 peptide, control M54 peptide, or saline at the indicated time points. **B.** Bar graph indicates frequencies of $CD103^{+}CD8^{+}$ T-cells that produce granzyme B under the indicated restimulation conditions. Pooled data are presented as mean ± SD of two independent experiments using four animals in control (i.e., saline or M54) groups and six animals in the AI9 restimulation group. **$p<0.01$

Figure S1

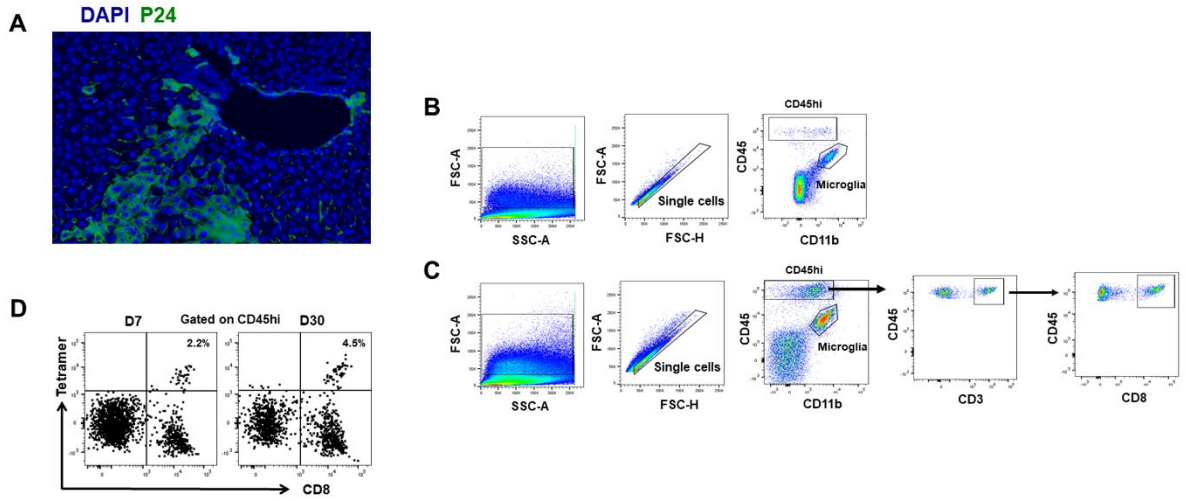

Figure S2

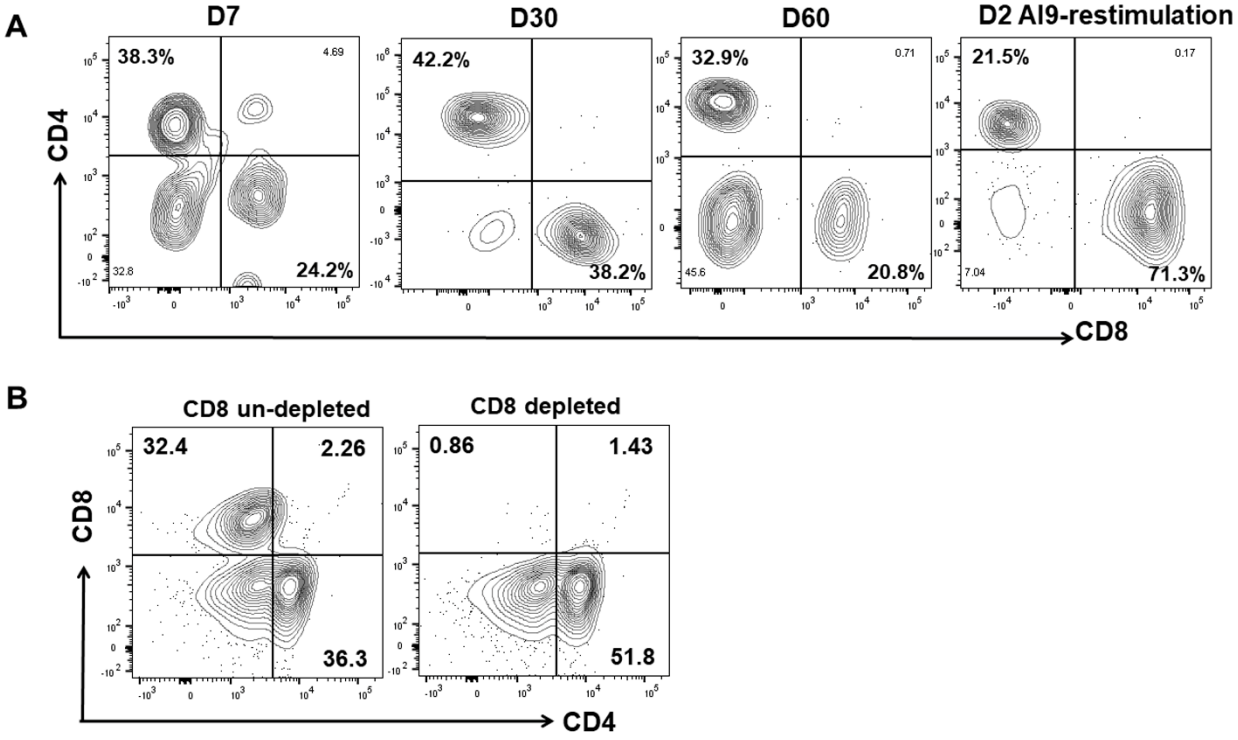

Figure S3

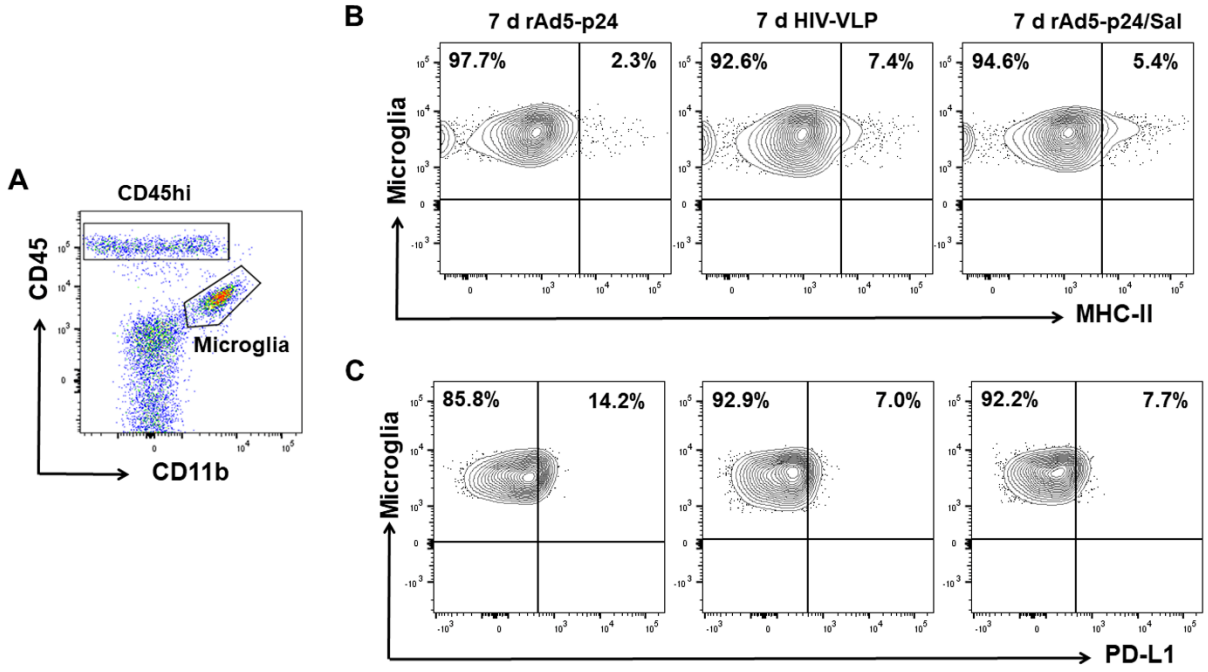

Figure S4